School of
Mechanical&Systems
Engineering

FABRICATION OF APATITE- WOLLASTONITE GLASS CERAMIC SCAFFOLDS BY 3D PRINTING

Written by

FATMA OZDEMIR

Supervisor

Dr. Oana Bretcanu

August 2015

DECLARATION

ABSTRACT

Skeletal defects, which are caused by trauma, disease, tumours or congenital defects, are healed by biomaterials with implantation into body. Bone has the ability to regenerate itself but it is up to small sizes. If the injuries are larger than the regeneration abilities of bone, then a biomaterial replacement is needed. The most popular solution are synthetic implants known as scaffolds that include the in vitro seeding and adhesion of cells on to porous structures and supply temporary service for stem cells to lead them differentiate into desired tissue[1]. A scaffold which directs cells to form functional tissue is usually used to replace into bone to supply tissue ingrowth[2]. Types of scaffold are ceramics, polymers and composites but it has been seen that ceramic-based scaffolds are brittle and polymers do not have high mechanical strength to mimic bone structure. However, glass-ceramic scaffolds are bioactive and have higher mechanical strength, osteoconductivity and osteoinductivity. Not only the material of scaffold is important, but also the fabrication technique of scaffold is crucial. 3D printing fabrication method allows to design desired dimensions and controlling mechanical properties[1, 3]. In present study, A-W glass ceramic scaffolds were fabricated by 3D printing technique and they were sintered to consolidate their structures. Bioactivity of A-W scaffolds were observed performing the bioactivity tests analysing the biodegradation rate and pH variation. At last, characterisation of the scaffolds was performed under SEM. However, biodegradation rate varies with respect to soaking days. After 1st week soaking period, it has been analysed that mass weight of scaffolds started to increase and scanning electron microscope characterisation results showed apatite-like layer started to form since 14 days of soaking in SBF.

ACKNOWLEDGEMENT

I am really grateful that I managed to complete this master program with all the supports that given from my supervisor, friends and family.

Firstly, I would like to thank my supervisor, Dr. Oana Bretcanu, that she gave me all her support and guidance to do this study as perfect and to improve my ideas, experiment and analytical skills. She was always optimistic and encouraged me when I felt stressed and hopeless. I could not have imagined having a better supervisor.

I owe my thanks to Stephen Moore for being helpful and supportive during my laboratory work. He always cheered me up when I was disappointed due to results.

My sincere thanks also go to the ‘kitchen crew’ (Grand Hotel), Alanood Alsowaidi, Atakan Bilgin. All those friends supported me while writing my thesis. The always motivated me nights and days.

I would like to express my gratitude to my family for supporting me spiritually throughout writing my dissertation.

Table of Contents

List of Tables

List of Figures

ABBREVATIONS

3D – Three Dimensional

2D – Two Dimensional

3DP-3D printing

CAD/CAM - Computer-Aided Design and Manufacturing

CaP - Calcium Phosphate

MD- Maltodextrin

Ca – Calcium

Si- Silicon

P- Phosphate

HCAp - Hydroxycarbonate Apatite

SBF - Simulated Body Fluid

AM - Additive Manufacturing

RP - Rapid Prototyping

SFF - Solid Free Form Fabrication

SLA – Stereolithography

SLS - Selective Laser Sintering

FDM - Fused deposition modelling

SEM – Scanning Electron Microscopy

SD - Standard Deviation

EDS-Electron Dispersive Spectroscopy

BTE-Bone Tissue Engineering

A/W – Apatite/Wollastonite

mL- Millilitre

dH_2O- Distilled Water

μm- Micrometer

wt%- Weight Percentage

TE- Tissue Engineering

SBF- Simulated Body Fluid

PLLA- Poly (L-lactide) acid

PGA- Poly (gycolic aci

1 INTRODUCTION

Most of the skeletal tissues are capable of doing self-repair naturally. For instance, patients own local cells can repair bone injuries up to critical size of fractures which are fractures between 2% and 10% of the strain and healthy tissue can form a new bone in this way with its osteoblast cells[4, 5]. However, prolonged rehabilitation or several procedures might be needed for traumatic fractures of the lower extremities, which are orthopaedic injuries to have successful recovery. Mostly, median age of the population has been suffered from bone disorders. Bone grafts, which are also known as synthetic biomaterials, have been designed to recover damaged organs and tissues to supply cell-materials interaction to be able to promote osteoconduction and to supply mechanical loading[6, 7]. These materials must have some mechanical and biological properties to restore injured tissues and to induce tissue growth as well. Therefore, scaffolds have been tailored to be porous, biodegradable, and bioactive and have appropriate Young's modulus[6-8].

Tissue injuries or diseases, which cause skeletal tissue losses, reduce quality of life at significant socioeconomic cost. According to researches along US and EU countries fractures approximately cost €17 billion and $20 billion annually respectively[9]. Approximately half of the hip replacements arthroplasty which is a procedure, need a revision and bone graft material is needed to augment host bone stock and to enhance the osteointegration with the native bone[10]. Mostly, skeletal tissue diseases such as osteoporosis, osteoarthritis, etc. affect elderly people and applied techniques cannot fulfil the expectations of patients. Novel area of tissue engineering suggests microarchitecture tissue engineering scaffolds that could be designed by 3D printing. These 3D printed scaffolds are assumed to mimic natural bone properties such as strength, stiffness and density. Scaffolds supply cell attachment and migration, transfer cells and biochemical factors, allow diffusion of cell nutrients and stimulate tissue ingrowth and replacement[1, 8].

However, scaffold mechanical properties must still be improved to sustain mechanical loading. 3D printing is a novel technique to print porous scaffolds

with designed dimensions to prevent poor mechanical properties and to sustain fast fabrication[6]. Not only the printing technique is important but also type of material (such as ceramic, polymer or composite) is crucial to sustain necessary requirements for scaffolds.

1.1 Scope of Thesis

The key goal of this research work is to fabricate porous apatite wollastonite glass-ceramic scaffolds for bone regeneration using 3D printing technology.

1.2 Objectives

- To fabricate the A-W glass ceramic scaffolds with powder based 3D printing machine
- To gain better mechanical and biological properties with this technique using CAD design
- To obtain porous 3D structures
- To sinter the green parts and densify the structures, then to analyze the effect of the sintering process on the dimensions.
- To evaluate the biodegradation rate of scaffolds after soaking in Simulated Body Fluid
- To observe the apatite-like form on the surface of scaffolds with SEM

2 LITERATURE REVIEW

2.1 Tissue engineering

Tissue engineering is a multidisciplinary branch in science especially in biomedical engineering, which combines information from material science, chemistry, biology, physics, engineering and medicine. Moreover, to overcome diseases, organ losses, bone and tissue regeneration, tissue engineering is a significant field. It mostly focuses on creation of organs, porous scaffolds and tissues[11, 12].

Tissue engineering aims reconstruction, improvement and maintenance of tissue function and provides regeneration with combination of stem cells, biopolymers and growth factors as can be seen in Fig1. Mechanical loading is thought as an essential requirement for scaffold fabrication in tissue engineering to mimic the structure that will be implanted in the body[9, 12].

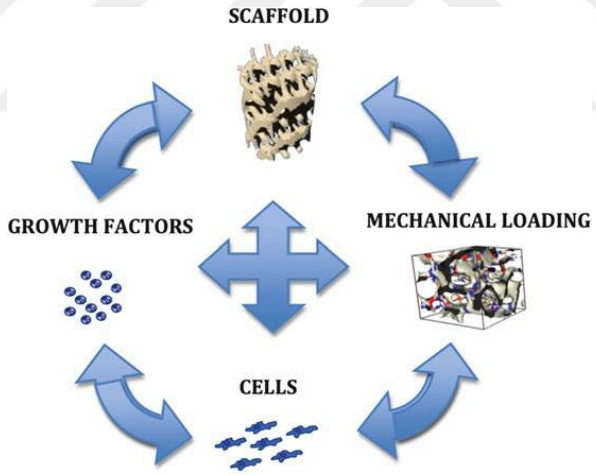

Figure 1: Construction of tissue engineered biomateria[13]l.

2.1.1 Bone Tissue Engineering

Bone tissue engineering seeks to enhance remodeling of the bone with differentiation and proliferation of cells, which are enhanced by cell migration and osteoconductivity using biomaterials. Therefore, scaffolds are used to direct cells to regenerate bone ingrowth. This process has applied with scaffolds combining growth factors, stem cells and drugs as can be seen in Fig1[2, 8].

Bone scaffolds have been used as a carrier to transfer nutrients and oxygen to cells and waste carried out from the cells. Growth factors and cells are melded into the scaffold to sustain cellular activity and tissue in-growth when it is implanted in the body. The porous structures of the scaffolds sustain tissue growth in it as well and at the same time scaffolds supply mechanical load[11]. Ashby et al. defines the importance of porous structures in nature as "when modern man builds large load bearing structures, he uses dense solids: steel, concrete, glass. When nature does the same, she generally uses cellular materials: cork, wood, coral. There must be good reason for it.[14]"

As process, cells are harvested from a donor and degraded into individual cells. These cells are seeded into scaffolds and implanted into tissue of the patient in which place is needed. To tailor suitable scaffold for bone, firstly bone structure must be known very well to be able to mimic bone tissue and creation of suitable environment for cell proliferation and maintain, as well as 3D geometry of scaffolds should be sustained[13, 15]. Recently, new emerging techniques are invented to overcome limitations of conventional techniques such as gas foaming, fiber bonding, melt moulding, solvent casting and particulate leaching to be able to create 3D geometric scaffolds and enhance cell attachments and proliferation. These techniques are computer control rapid prototyping techniques that aims to create precise geometric structures[16].

2.2 Bone Structure

Bones are rigid frameworks of the body that protect and support soft tissues and vital organs. They are lightweight, highly vascularized and contain minerals as well[9]. Basically; bone is formed by compact and cancellous bone. Cortical bone (figure 2), which is known as compact bone as well, is strong, dense and tough including osteons, osteoblasts, and osteocytes. Porosity of the cortical bone is approximately between 5-10% and it is placed at the outer shell around cancellous bone. Cancellous bone (figure 2) is known as trabecular that is lighter, less dense and more porous than compact bone approximately between 50-90%, and has red blood cells, osteoblasts, platelets and white blood cells.[8] Bone is naturally formed of collagen and hydroxycarbonate apatite with 10-30% porous hard outer layer (cortical) and 30-90% porous interior (cancellous) [7, 17, 18]. Therefore, mechanical properties of bone differ from cortical bone to cancellous bone. Hence, the designing of the ideal scaffold is not easy.

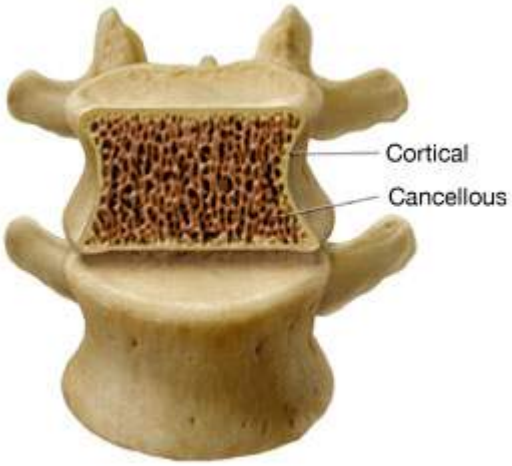

Figure 2: Cortical and compact bones[19]

2.2.1 Bone Cells

Bone has a dynamic structure and it can heal itself with its bone cells up to critical size that is a few millimeters distance from the healthy bone [12]. Osteoblasts, osteocytes and osteoclasts are the crucial cells for regeneration of the bone. Osteoblasts are formed from mesenchymal stem cells and they synthesize bone matrix to form new bone cells. Osteocytes are inactive osteoblasts and situated deep in bone matrix. In contrast, osteoclasts are responsible to break down the bone and these cells are generated from monocyte stem cells. While osteocytes

and osteoblast cells are working together, they form new bones naturally[7, 12, 20].

2.3 Scaffolds

Scaffolds are temporary templates to sustain cell adhesion and mimic the extracellular matrix to provide structural reinforcement for neotissue, which is new tissue around the scaffold[21]. Scaffolds have been developed to overcome limitations and disadvantages of bone allografts and autografts[1]. An allograft is the tissue that is harvested from a donor patient and then implanted into the host patient's body. An autograft is the tissue that harvested from the host patient's healthy tissue then implanted into host patient's body again to repair the defect. In the previous section, it has been mentioned that scaffolds are melded with biological markers, growth factors and stem cells to be implanted into injured tissue to supply tissue ingrowth on it and bone regeneration will be completed. The matrix which is a scaffold, supplies specific appropriate environment for cells architecturally, mechanically, biologically and it transfers the necessary materials. Architecture of a scaffold is also important to supply cell adhesion on its porous matrix. This temporary matrix guides cell proliferation and differentiation until the new bone is regenerated. Furthermore, cells need nutrients and oxygen to grow properly. Thereby, scaffolds serve as carriers to transport nutrients, gasses and growth factors for cells to lead them through to scaffold and to help recovery healthy cell function as well[2]. Metabolic wastes such as carbon dioxide are transferred out from the scaffold[13]. On the other hand, if all the transport systems does not work properly it will cause the cell to drive. Therefore, an ideal bone scaffold must supply migration, differentiation and proliferation after meeting all the requirements. Interconnectivity between porous structures shows excellent ability to create a place for tissue ingrowth[2, 3, 9]. Furthermore, it is important to fabricate controllable, reproducible, cost effective and 3D structural scaffolds with appropriate mechanical and biological properties[2]. Selection of the materials is also significant to design scaffolds with necessary biomechanical properties. Generally, polymers, ceramics and composites are used in tissue engineering scaffolds.

2.3.1 Biological and Mechanical Requirements for Scaffolds

Biocompatibility, which is one of the most important properties for a material is defined as continuation of cellular activity without causing any toxicity into the tissue. Beside the biocompatibility, scaffold must be osteoconductive to sustain integration between bone cells and the surface material that cells will adhere onto surface and start to proliferate and form extracellular matrix. Moreover, an ideal scaffold should be osteoinductive as well to form a new bone via bimolecular signaling and recruiting progenitor cells. Blood vessels will be formed through scaffolds to supply nutrient, oxygen and waste transport[2, 3, 7]. Bioactivity is another crucial requirement for scaffolds that form an interfacial bond with the biological tissue. In vitro and in vivo studies showed that bioactive materials react with tissue fluids, promote precipitation of hydroxyl apatite on the material surface. Bioactivity test is performed to observe bioactivity for in vitro studies with simulated body fluid solution[3, 7, 9].

Scaffolds have to mimic mechanical properties of bone and should have a good load transfer. Cancellous and cortical bones have different mechanical properties. For example, a cortical bone has 15-20 GPa Young's modulus and between 0.1-2 GPa is for a cancellous bone. Furthermore, compressive strength of the cortical bone is between 100-200MPa and it is between 2-20 MPa for the cancellous bone. Thereby, the challenging part is to cover all mechanical property requirements for both bone structures[9, 20].

Another property of an ideal bone scaffold is porosity that is a really crucial requirement. It sustains significant benefits for cellular activity such as diffusion of nutrients, gasses and waste removal via pores but the size has to be minimum 100μm in diameter. According to literature studies, to obtain the maximum efficiency for tissue ingrowth, pore size should be between 200 and 350 μm. On the other hand, it can sustain some disadvantages as well. Porosity decreases mechanical properties through reducing compressive strength and increase the complexity to reproduce scaffolds[12]. At the same time, increasing the porosity of the scaffolds increase the surface area and it favors bioactivity, resorbability and osteoinductivity of the bioceramic scaffolds[22, 23].

Basically, to obtain more efficiency from a scaffold, macroporosity (between 300-

500μm) sustain bone growth and vascular growth. Microporosity, which is less than 50μm, is crucial for osteointegration, cell and protein adherence and cell migration. Interconnectivity supplies cellular migration, nutrient diffusion and neovascularization[17].

Some studies showed that bioactive glass scaffolds should have at least 50% open porosity to allow tissue ingrowth, microporosity should be higher than 300μm, interconnectivity between pores should be between 50-100 μm that is the minimum value to permit vascularization of the scaffold and for functional scaffolds microporosity should be less than 10 μm. Effects of pore sizes on tissue growth is showed in Table 1

Table 1: Pore size and effects on the tissue[24]

Pore Size (μm)	**Effect on tissue ingrowth**
5 μm	Neovascularization
5-15 μm	Fibroblast ingrowth
20-125 μm	Regeneration of adult mammalian skin
10-100 μm	Osteoid growth
100-350 μm	Bone regeneration
500 μm	Fibrovascular tissues for rapid vascularization and survival of cells

Degradation of biomaterials in the living body is proportional to the healing tissues which is crucial to allow the new bone information. This property is known as bioresorbability, which supplies bone regeneration. Porosity and micropores can affect the degradation rate straightly[1, 25]. In figure 3, it can be seen that when tissue ingrowth starts, scaffold degrades slowly by the time of healing and new tissue cells fill pores. Thus, new mature bone occurs[9].

Figure 3 Stages of bone remodelling by replacement of scaffold[9]

2.3.2 Types of Scaffolds

2.3.2.1 Polymer based scaffolds

Natural polymer based scaffolds are collagen, fibrin, chitosan and starch. These kind of polymers can be easily designed and they can sustain osteoconductivity very well. However, their mechanical strength is not high to mimic natural bone and beside this, polymers degradation rates are very fast. Synthetic polymers can be fabricated with appropriate temperature, pressure and dimensions that is easier than fabricating natural polymers. Therefore, this kind of polymers can have reproducible properties mechanically and physically, which are degradation rate, tensile strength and young's modulus. However, during degradation process synthetic biodegradable polymers release acidic products that causes a reduction in mechanical strength[2, 3, 12].

2.3.2.2 Ceramic base scaffolds

Ceramic-based scaffolds have higher biocompatibility and they can sustain better bone-biomaterial integration. Mechanically they can mimic the bone and generate bone-apatite like materials on the surface of the scaffolds. As another advantage they are neither cytotoxic nor antigenic. However, ceramics are brittle and they have low degradation rates. Bioinert ceramics, which are alumina and zirconia can be fabricated to be used for hard tissue repairing in non-porous form. Bioactive ceramics such as glass-ceramic, bioactive glass and HA, can be used to enhance integration between bone and biomaterial. Bioactive glasses are resorbable, biocompatible, osteoconductive and osteoinductive[12, 15].

2.3.2.3 Composite based Scaffolds

Combination of two materials usually offer better mechanical properties that mimic the natural bone structure than the single component material. Composite scaffolds are polymer-bioceramic scaffolds used to enhance mechanical properties, improve osteoconductivity and have controlled degradability[6, 12].

In this project, apatite wollastonite glass ceramic scaffolds will be analyzed. Studies have showed that it there is a high integration rate between scaffold and bone. Moreover, A-W glass ceramic has better fracture toughness than ceramic and glass phases. It will be an excellent choice to avoid propagation of cracks and to prevent being distorted. This bioactive glass-ceramic scaffold has better osteoinduction properties and biodegradability[7, 15, 26].

Apatite is a group of phosphate minerals and it includes hydroxyl apatite, fluorapatite and chlorapatite. In the crystal structure, it involves high concentration of OH^- , F^- and Cl^-[27].

Wollastonite is a group of silicate mineral which is a calcium mineral ($CaSiO_3$) and it is usually white. Small amount of magnesium, iron and manganese is found in its structure[27].

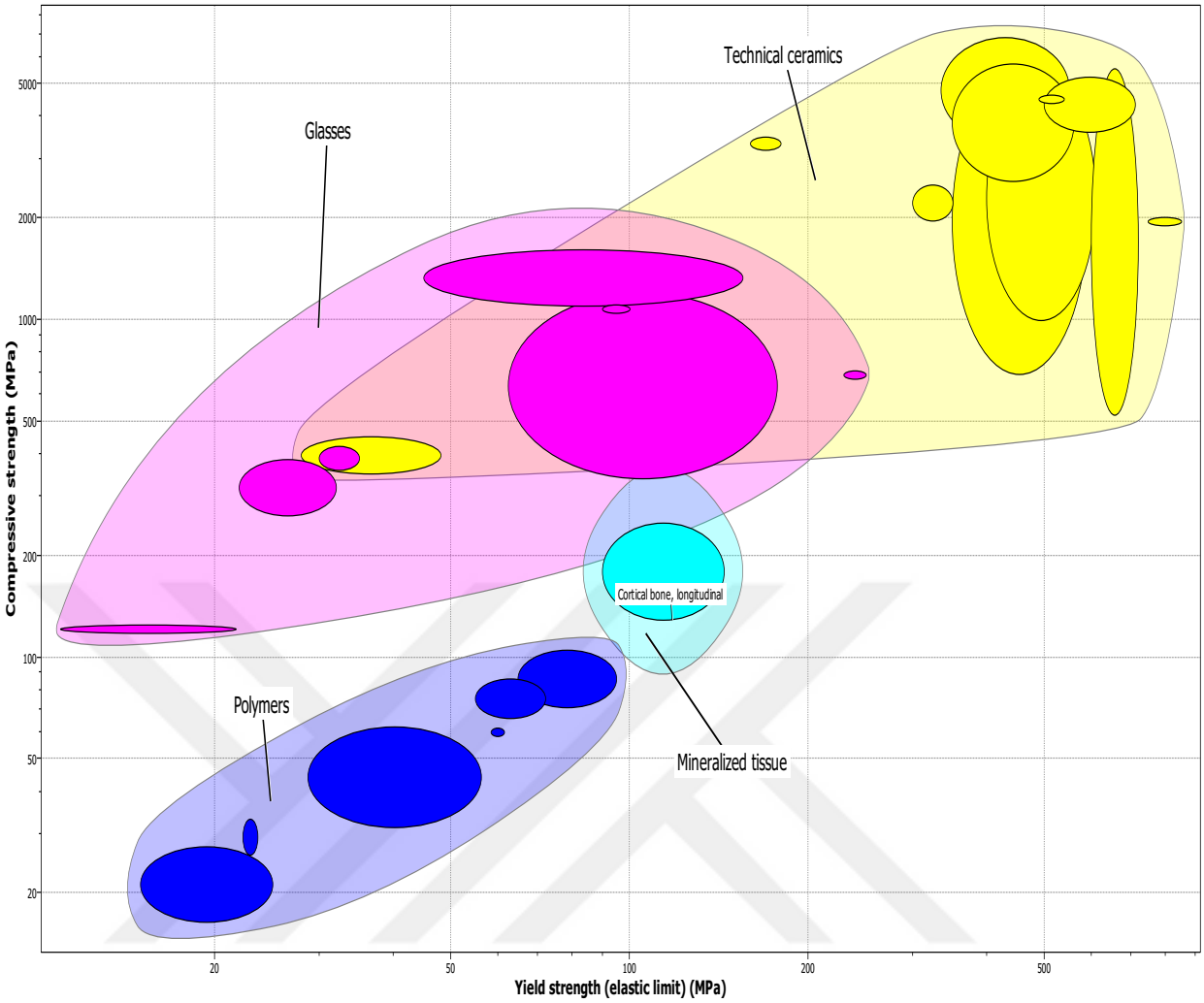

Figure 4: Mechanical properties comparison of polymers, bone, glasses and ceramics for biomedical purpose[28]

According to figure 4, ceramics and glasses have higher compressive strength and yield strength values compared to polymers Yield strength and compressive strength values of the cortical bone is similar to that of glasses and ceramics. Glass-ceramic scaffolds share properties of glasses and ceramics and fabricated through controlled crystalline of base glass. Thus, they have high strength, toughness, high temperature stability, biocompatibility, resorbability and bioactivity.

2.3.3 Fabrication Methods

2.3.4 SOLID FREE FORM

Computer-aided design (CAD) is used to design 3D complex structures. As can be seen in figure5, different shapes and designs could be designed with the software easily[29].

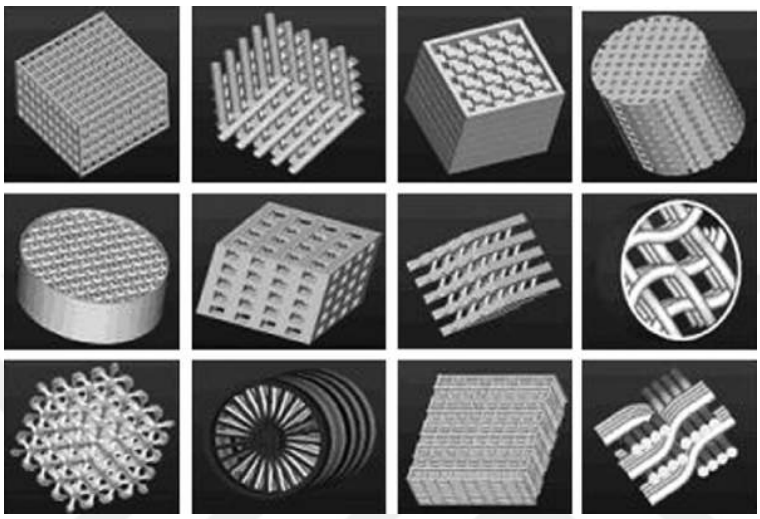

Figure 5: Example of different designs of scaffolds[30]

Computer aided design is a new concept of computer aided tissue engineering that is used to create scaffolds with desired dimensions and shapes to be implemented into body (Fig5). This method provides better mechanical and biomechanical properties so they can be designed and applied easily. 3D complex geometric samples can be manufactured with the exact same physical structure of the samples[13, 29] .

Additive manufacturing techniques are performed with CAD to manufacture the scaffolds with appropriate mechanical architectural properties. As principle, these kind of techniques fabricate the scaffolds layer by layer. As an advantage, these techniques supply freeform fabrication of scaffolds[7, 13].

Additive manufacturing is not the only way to fabricate scaffolds. Solvent casting and particulate leaching, melt molding, fiber bonding and gas foaming can also be performed as indirect scaffold fabrication methods. However, most of the studies have showed that there are too many limitations. Traditional methods cannot fulfill the expectations mostly because of poorly controllable pore size, pore shape, interconnectivity, and geometry of samples. Porosity properties

have significant effects on mechanical and biological features of scaffolds. Although some of the conventional methods are able to create an interconnected microporosity tissue engineering scaffold they are usually without precision and reproducibility[1, 6, 29].

Solvent Casting and Particulate Leaching

This technique is a frequently used, easy and inexpensive technique to develop scaffolds such as bioactive polymer-ceramic structures. Basically, scaffold is prepared by evaporation of the solvent according to Mikas et al. technique. To create a layer of polymeric membrane, a synthetic polymer PLLA is added into organic solution that includes chloroform and porogens such as salt to form pores. The composition is soaked in water to gain porous structures[31]. Polymer solvent is removed with freeze-drying method. Good porosity results can be gained with this technique. Desired dimension of pores depends on shape, size and amount of porogens. However, the highly toxic solvent is used, reproducibility is to low and it has limitations whilst producing desired dimensions, pore shape is not easily able to design as desired[9, 12].

Melt Molding

This technique is usually used in combination with other methods because of fibres production. Teflon mould is used to gain the desired shape. A mixture of fine PLGA polymer powder and gelatin microsphere is filled into the mould with porogens and it is heated to high temperature above the glass-liquid transition temperature of polymer where the synthetic polymer particles bond together. After the mould is removed, composition is immersed in water to create pores[31]. This method does not contain toxic solvent to remove porogen, however high temperature is necessary for non-amorphous polymer. Porosity, pore size and macro shape can be controlled in this method[9].

Fiber Bonding

Mikos et al., found the fiber bonding technique that involves woven or knitted fibers. Synthetic polymer PLLA solution is used to immerse aligned PGA fibers then solution is heated above the melting temperature of PGA and PLLA polymers and the solvent is allowed to evaporate. Only PGA fibers are left after removing of PLLA with selective dissolution.

This technique provides a large surface and great interconnectivity, thus cell adhesion and nutrients' transport can progress easily. On the other hand, pore size and porosity cannot be controlled and remnant solvent affects cells badly.

Gas Foaming

Biodegradable polymer disks are exposed to high pressure of CO_2 (800 psi) to be saturated, then the pressure of CO_2 is decreased to atmospheric level to lower the solubility of the gas in the polymer. This technique provides pore sizes to be between 100μm and 500μm. However, the mechanical strength of scaffolds are not efficient[31, 32].

When all the limitations has been considered direct fabrication methods have been emerged to overcome enhance the architectural, mechanical and biological properties of scaffold.

Solid free from fabrication technique is known as rapid prototyping and additive manufacturing as well whose types are 3D printing (3DP), selective laser sintering (SLS) and fused deposition modeling (FDM). When these techniques compare with indirect methods, major limitations such as lack of reproducibility and absence of interaction has not been observed.

Selective Laser Sintering

It is a heat-based technique that spread layer of powder by a roller scanned by CO_2 laser beam which supplies energy to increase the temperature. Material is started to heat above the material's melting temperature to fuse the particles and form 3D scaffolds in defined shapes. After fabrication of one layer, platform is lowered and another layer is spread to be fabricated iteratively[16, 33].

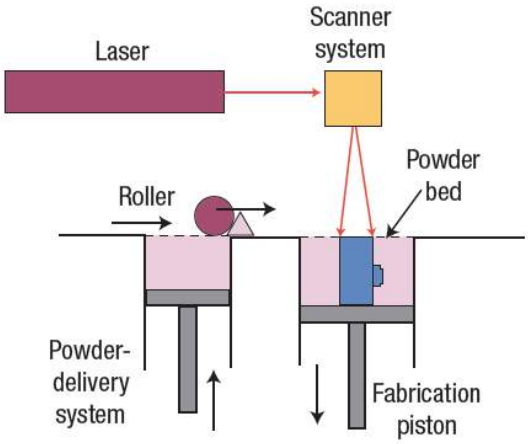

Figure 6: Schematic description of Selective Laser Sintering[34]

Fused Deposition Modeling

This technology is based on an extrusion system. A heated-head extruder pumps the thermoplastic material through nozzle onto the build platform and fabrication of scaffold is started. Platform is moved down in the z-direction after fabrication of one layer and then other layers are fabricated. It is a layer by layer 3D scaffold fabrication process. Layer thickness depends on diameter of the nozzle.

A good melt in a viscosity property is important for this technique. Materials are limited to be thermoplastic materials and in addition to ceramics[2]. It does not need solvent like other techniques and it is an effortless process[9]. Pore sizes can vary between 250-700 μm[16].

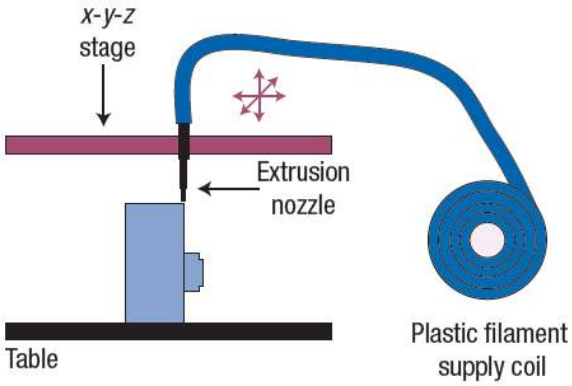

Figure 7: Schematic description of fused deposition modelling

2.4 3D PRINTING

As it has been mentioned in the previous section, 3D printing is a type of additive manufacturing method known as powder-based freeform fabrication technique with using CAD. 3D printing is a powder based fabrication method that was invented at the Massachusetts Institute of Technology, USA in 1992 to print designed materials made of ceramics, polymers and metals[7].

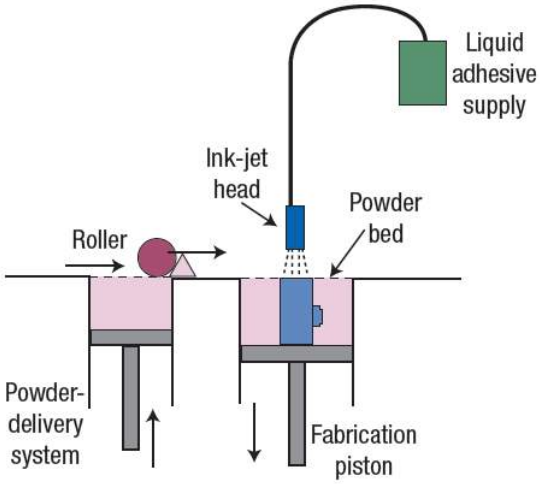

Figure 8: Powder based 3D printing

As can be seen in the Figure 8: Powder based 3D printing, powder based 3D printing has two platforms, the powder is placed onto feed piston and will be spread through to build piston with a gantry (roller). When the platforms reach the same thickness, fabrication of scaffolds started dropping binder

automatically. Binder binds to granules as the defined structure and the first layer is started to be fabricated. Then the new layer of powder covers the fabricated layer and binder drops again to fabricate the fresh layer. This process is repeated until the defined 3D scaffolds are produced. This technique can be defined as layer-binder-layer method as well. Printed scaffolds are left into the device over night for drying. Later, they are collected and the unbound powder is removed by airflow[7, 22].

3 Materials and Method

Recently, apatite wollastonite scaffolds have been started to be used mostly due to their high bioactivity and mechanical strength properties. In this study, less than 53μm grain size of apatite wollastonite was developed with maltodextrin powder to print green parts. MD is used as a binder which is a polysaccharide and it is biocompatible for ceramic scaffolds as well. MD acts as an adhesive to bind the apatite wollastonite powder when triggered by liquid powder[35]. Rapid prototyping is a fast and cheap method which provides printing of physically complex 3D materials. A-W and Maltodextrin powder mixture were printed with powder based on 3D printing. Bioactivity tests were applied to observe bioactivity and biodegradation rate of A-W scaffolds. Materials and methods of study will be described in detail at this part. Steps of the methodology can be seen in Figure 9.

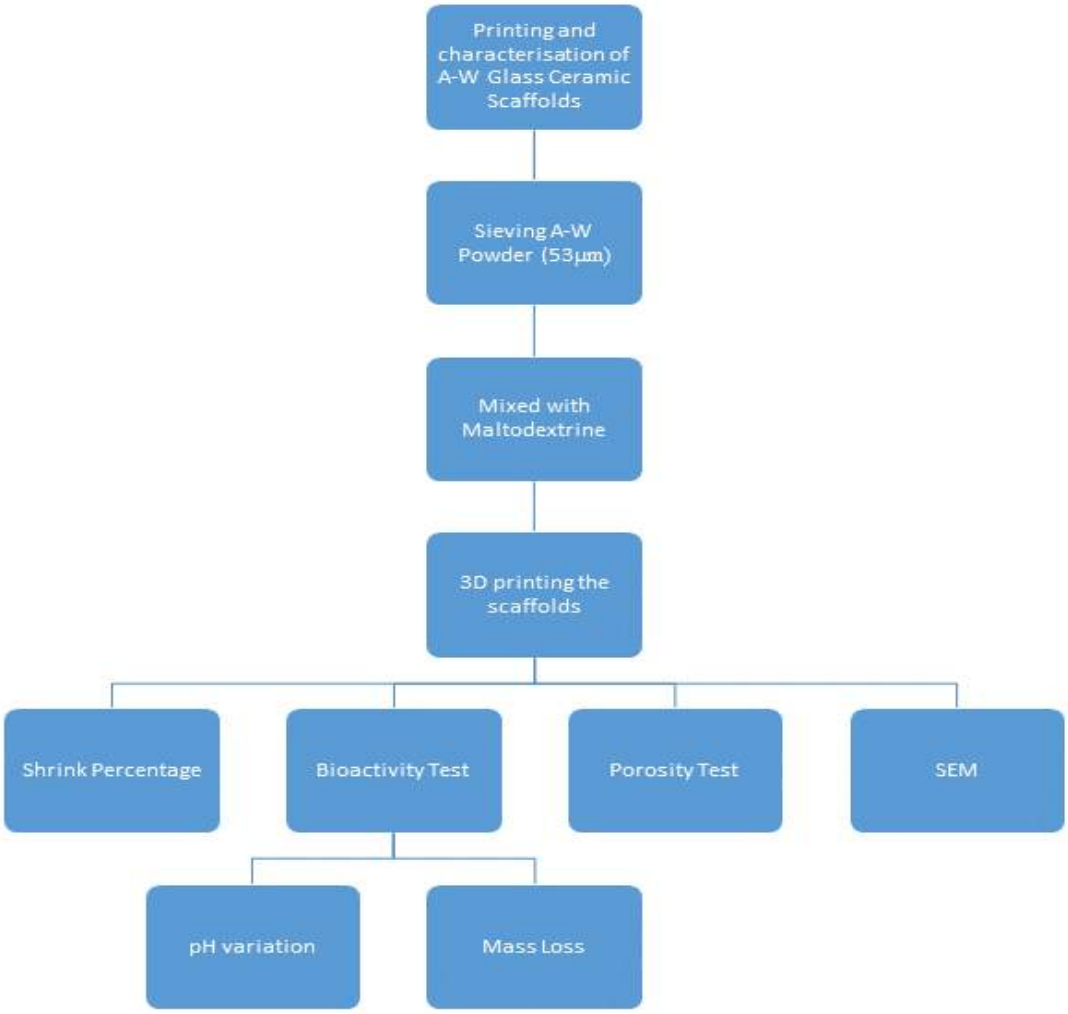

Figure 9: Procedure of the present study

3.1 Specimen Preparation

3.1.1 Sieving Process

Apatite Wollastonite glass ceramic powder (GTS, Sheffield, UK) were sieved with less than 53µm particle sizes by auto sieve shaker (Impact, UK) (Figure 10) to obtain a particular grain size of powder. In total, 280 grams of powder were collected after sieving

Figure 10 : Auto sieve shaker to sieve less than 53µm grain size of A-W powder.

3.1.2 Weighing the Powder

Ditigal scale (Figure 11) was used to weight totally AW and MD powders separately to obtain 400 grams of mixture. Both powder were weighed in ratio of wt% 70:30 by mass. Separately, 280 gram of A-W powder and 120 gram of Maltodextrin powder (Oneon, UK) were weighed and placed into a plastic bottle. Generally the suggested amount for 3D printing is between 350 and 500 grams to print the designed 3D scaffolds. Digital scale was used again to weigh the reagents of SBF solution.

Figure 11: Digital scale to weigh the samples

3.1.3 Mixing A-W and MD powder

Weighed A-W and MD powders were placed into a plastic bottle in ratio of wt % 70:30 by mass and analogue tube rollers (Stuart, SRT6) were used to mix the powders of fixed speed to sustain rocking and rolling actions. (Figure 12)

Figure 12: Rolling machine to mix maltodextrin and apatite wollastonite

3.2 Fabrication of the Scaffolds

3.2.1 Designing the Structure

Scaffolds were designed in desired shape and dimensions using Autodesk Inventor Professional, U.S (Figure 13) which is a computer aided design software program to design and visualize 3D prototype structures. 42 Scaffolds were created with 10.25mm diameter and 2.25mm in thickness as cylinder in Z-axis using the software. The file was saved as a *STL file and directed to 3D printing.

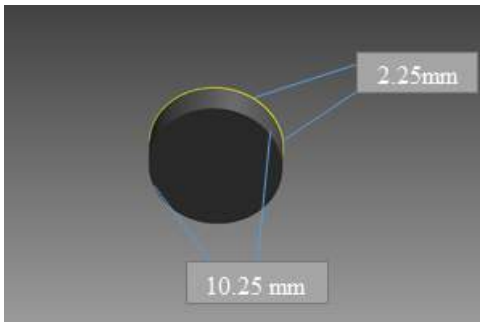

Figure 13: A designed scaffold in Inventor software program

3.2.2 Printing the Scaffolds

Powder-based 3D printer (ZPrinter 310 Plus, USA) was used to print A-W glass ceramic scaffolds with a 70% A-W – 30% MD, layer by layer. Before starting the fabrication process, the samples and the 3D printer were prepared step by step. As it can be seen in Figure 14, feed piston was down and built piston was set up by pressing the up and down buttons on the control panel. The mixture of A-W and MD powder were placed onto feed piston. Powder was upturned with propylene scraper (Figure 15) and gathered together to remove air and to make the powder firm. Powder was carefully compressed with Tamper (Figure 15) to make the surface completely smooth and compact. To start printing, spread button was pressed 4 times on control panel and after the fifth press, Gantry (Figure 15) started to spread the powder from the feed piston to build piston and made powder layers on the build piston part. At the same time liquid binder was dropping onto the powder layer. As the liquid binder, zb*60 clear binder which is suitable for glass ceramic scaffolds, was used. When powder and liquid binder interacted, it hardened powder and created solid 3D scaffolds layer by layer, as can be seen in Figure 16.

Figure 14: Components of 3D printer (Zprinter 310Plus)

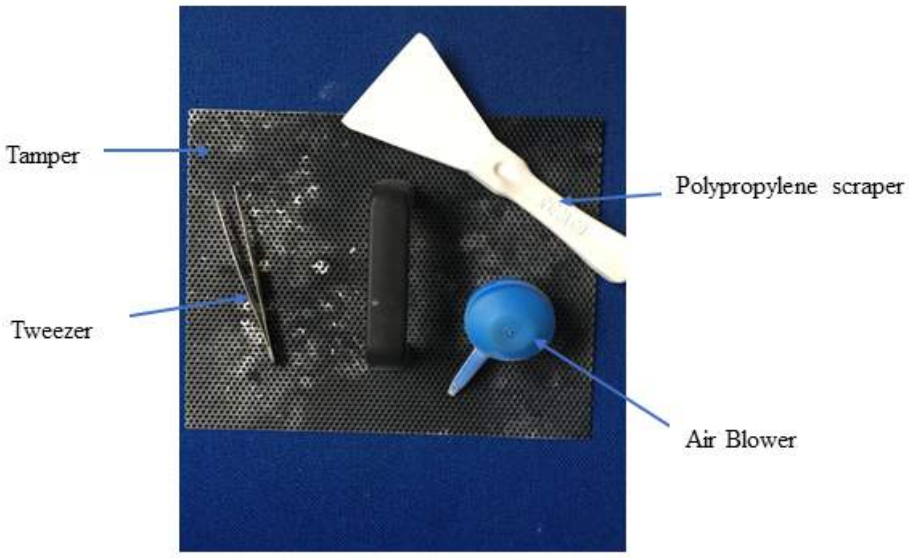

Figure 15: 3D printing Kits

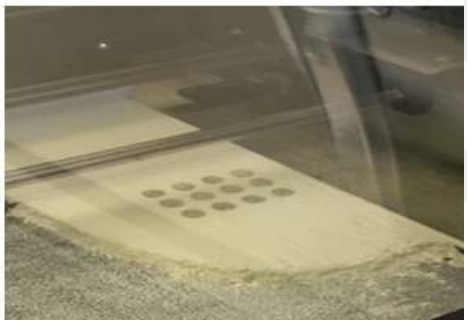

Figure 16: An example of printed scaffolds

After fabrication of the scaffolds, all the specimens were left for over to dry before removing them. The day after unbound powder was air blown with air blower (Figure 15) and a soft brush was used to remove the unbound powder to obtain porous structures.

3.3 Measuring the dimension of scaffolds

Dimensions of samples were measured with a digital caliper (Mitutoyo, UK) (Figure 17) before and after the sintering process, to analyse the effect of sintering process and the shrinkage percentages were calculated according to the dimension measurements of scaffolds.

Figure 17: Caliper (Mitutoyo, UK) to measure the scaffolds before and after sintering process

3.4 Sintering process

A-W glass ceramic scaffolds were sintered (Figure 19) into the furnace at 1150°C (Carbolite Ltd, UK) to densify the structure of scaffolds. High temperature makes structures denser and increases their mechanical strength. However, A-W glass cannot resist to too high temperature and melts because of its ceramic structure. Thus, platinum foil were placed underneath the specimens and two bricks were used. First stage was 800°C that increased 10°C per min for 1 hour to burn out the binder which was maltodextrin and second stage was 1150 °C with an increase of 10°C per min for 1 hour to sinter mineral deposits that can be seen in the Figure 18.

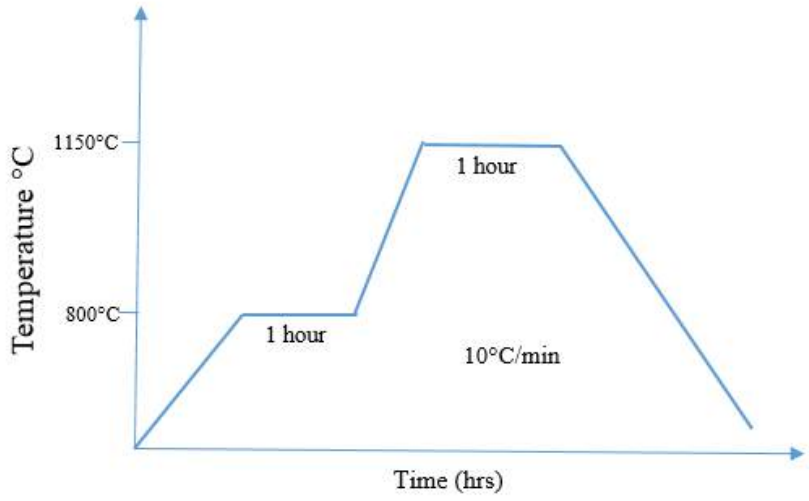

Figure 18: Sintering Conditions

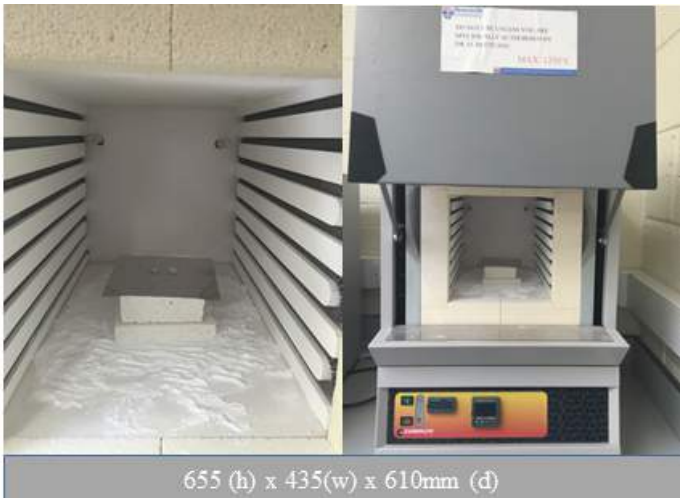

Figure 19: Furnace to sinter samples

3.5 Shrinkage evaluation

Sintering process was applied to increase the mechanical strength of scaffolds by applying high heat. During this process, scaffolds became denser and shrank. Shrinkage is crucial to analyse the effect of sintering and whereby, before printing the scaffolds' shrinkage percentage can be considered and designed using the software. Shrinkage percentage was calculated as linear shrinkage and volumetric shrinkage. Percentages of shrinkage were calculated for the scaffolds which were printed and designed in Inventor due the change in dimensions after the fabrication process.

Dimensions of scaffolds before and after the sintering process were measured with a digital caliper (Mitutoyo). Linear and volumetric shrinkage are calculated with the equations below;

$$\text{Linear shrinkage } (\%) = \frac{L1-L2}{L1} \times 100 \quad (1)$$

where L_1 represents initial length of the scaffold before sintering process and L_2 is the final length of the scaffold after sintering process.

The same equation is used to calculate the linear shrinkage of scaffolds because of the printing process, where L_1 represents the designed length of the scaffold and L_2 is the length of the printed scaffolds.

$$\text{Volumetric Shrinkage } \% = \frac{V1-V2}{V2} \times 100 \quad (2)$$

In the above formula, V_1 is the initial volume of the scaffold before sintering and V_2 is the final volume of the scaffold after sintering.

Volumetric shrinkage equation is applied again to calculate the shrinkage percentage of designed scaffolds and the printed scaffolds where V_1 is the volume of the designed scaffold and V_2 is the volume of the printed scaffolds.

3.6 Dry weight of Scaffolds

After the green parts were post-processed, dry weights of the samples were weighed with an analytical balance (Kern Analytical Balances, ABT 220-5DM) (Figure 20) before soaking them into simulated body fluid. Same process was applied after scaffolds were taken out from SBF. Weighing results were compared to observe the mass loss of the samples and analyse biodegradation rate.

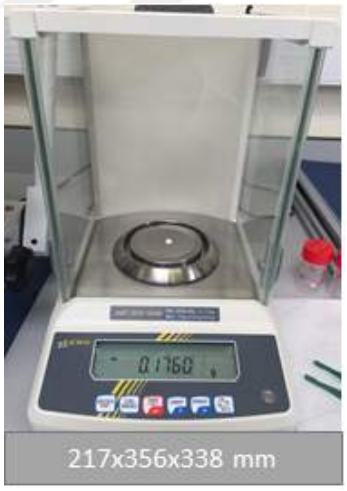

Figure 20: Analytical Balance to weight dry weigh of the scaffolds (Kern Analytical Balances, ABT 220-5DM)

3.7 Porosity evaluation

Porosity is described as the void space in a porous solid. The open porosity of scaffolds were measured with a digital scale (Kern analytical balance, ABT 220-5DM) and density kit (KERN AES-A01) shown in Figure 20 based on Archimedes' principle. After, measuring the dry weights of scaffolds, the scaffolds were suspended in water and weighed. As a second step, wet weights of the scaffolds were measured (Figure 21). Open porosity is calculated as;

$$\text{Open Porosity } \% = \frac{Ww - Wd}{Ww - Ws} \; x \; 100 \qquad (3)$$

where W_w is the wet weight of the scaffold, W_d is the dry weight of the scaffold and W_s is the submerged weight of the scaffold.

Figure 21: Digital scale to measure the open porosity of scaffolds, Density Kit (Mettler- Toledo, 2008)

3.8 Bioactivity in SBF

SBF that mimics the human blood plasma, was prepared with different ion concentrations according to Kokubo's formula (Table 2)[36].

Table 2: Regents for preparing SBF (pH 7.4, 1L)[36]

Order	Reagent	Amount
1	NaCl	7.996 g
2	$NaHCO_3$	0.350 g
3	KCl	0.224 g
4	$K_2HPO_4 \cdot 3H_2O$	0.228 g
5	$MgCl_2 \cdot 6H_2O$	0.305 g
6	1M-HCl	40 mL
7	$CaCl_2$	0.278 g
8	Na_2SO_4	0.071 g
9	$(CH_2OH)_3CNH_2$	6.057 g

700mL of deionized water (dH_2O) was filled in 1L of bottle as can be seen in Figure 22: Magnetic stirrer with heating to prepare SBF solution. Kokubo's formula (Table 2: Regents for preparing SBF (pH 7.4, 1L) were followed to prepare the SBF solution at 37°C with a 7.4 pH value. After adding each reagent, 20 minutes were waited for the ions to dissolve. To obtain the 7.4 pH value, HCl of 35mL was used at first and the remaining 5mL were added drop by drop while checking the pH value until it reached 7.4 pH value. After adding all reagents the bottle the solution was completed to 1L by adding dH_2O. The prepared SBF was kept in the fridge for two days.

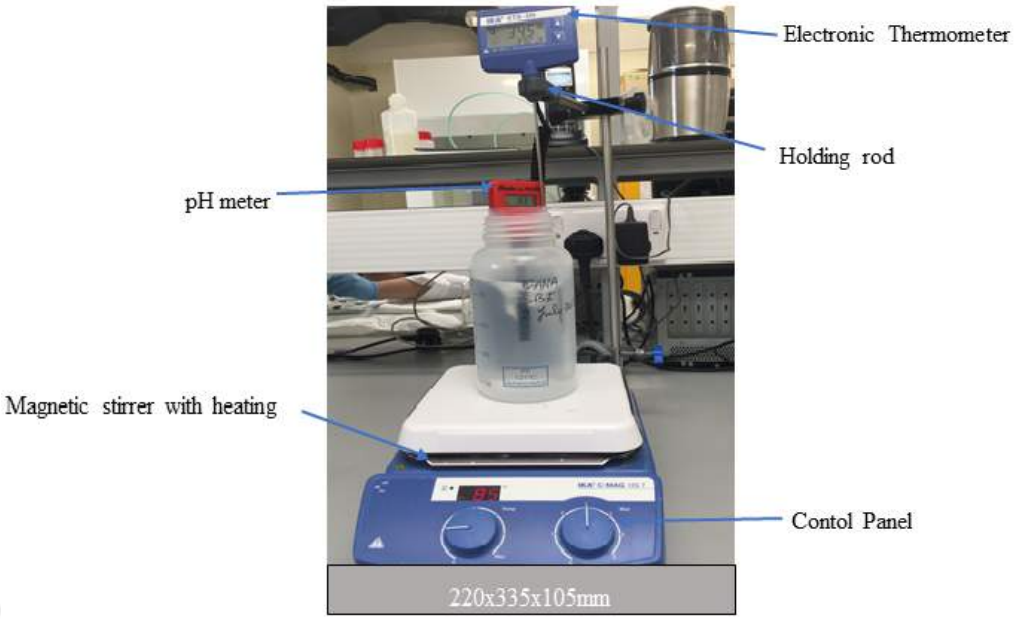

Figure 22: Magnetic stirrer with heating to prepare SBF solution

To soak the scaffolds in SBF solution, principally scaffolds were placed into small plastic containers. 10mL of SBF was then slowly added into each container. Plastic containers which had scaffolds were kept in the incubator to kept SBF solution at 37°C to mimic human body temperature.

Samples were immersed into the solution for 7, 14, 21, 28, 35, 42 days to observe bioactivity of A-W glass ceramic scaffolds in vitro test. SBF solution was refreshed every 3 days and scaffolds were removed from the solution weekly except for the 7^{th} group of the scaffolds that was kept in solution for 42 days without refreshing the SBF. In every 3 days before refreshing the solution, pH values were measured.

Removed scaffolds were dried at ambitious temperature for 2 days. Then, dry weight of the A-W glass ceramic scaffolds were measured and surface morphology of scaffolds were performed with SEM for visualising the apatite-like layer forming on the surface.

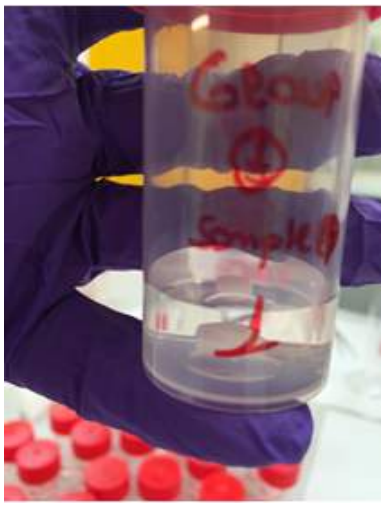

Figure 23: An immersed scaffold into the plastic container

3.9 Characterisation

SEM was used to analyse miscellaneous parts of the porous structure of scaffolds and to observe the apatite-like layer on the surface of the A-W glass ceramic scaffolds.

The scaffolds were placed on top of the metal disk with an appropriate height of disk for SEM for analysing as can be seen from the right image of Figure 24.

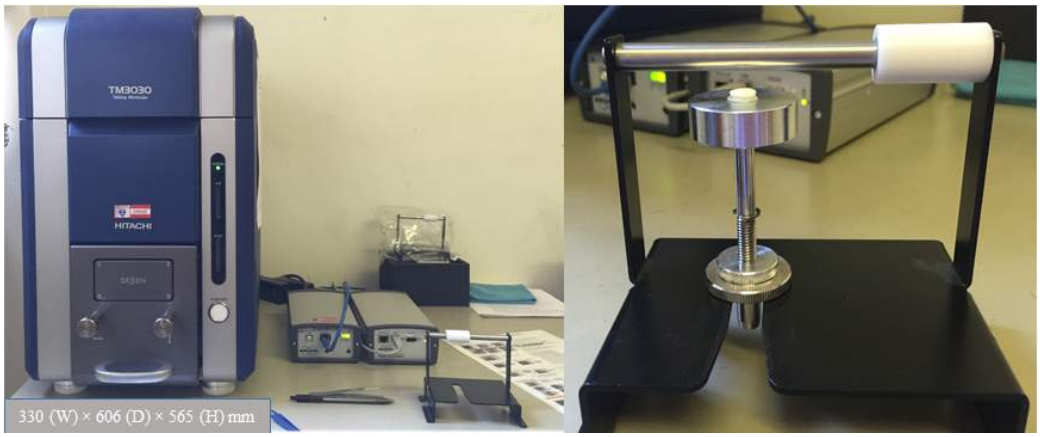

Figure 24: Scanning Electron Microscope

4 RESULTS

4.1 Effect of 3D Printing Process

3D printing is an emerging technique to provide good mechanical strength and fabricate uniformed A-W scaffolds. However, after fabrication of A-W glass ceramic scaffolds it had been seen that they did not have uniform structures as it can be seen in Figure 25.

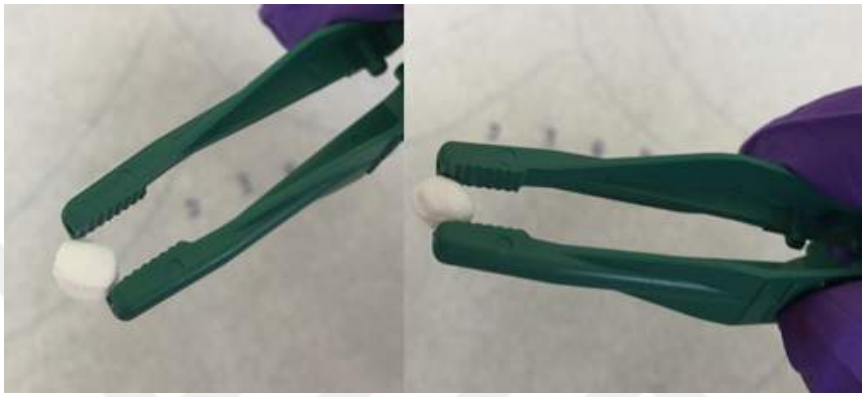

Figure 25: Structure of scaffolds

Scaffolds were designed in Inventor Software before the fabrication process. Dimensions of the scaffolds were 10.25mm diameter and 2.25mm length. However, after printing the scaffolds when they were measured with caliper (Mitutoyo, UK), it had been determined that dimensions changed.

According to the analysis, 3D printing process caused 2.09% of volumetric shrinkage resulted in equation (1) (Table 3). Designed scaffolds had 194.83mm^3 volume but after printing the scaffolds measurements showed that the volume of scaffolds were 190.76mm^3 as it can be seen in Figure 26. Linear shrinkage of the scaffolds is -19.11% (Table 3) which means thickness of scaffolds rose that was resulted in equation (2). It is a crucial changes in dimensions of scaffolds due to the printing process that should be considered before fabrication of scaffolds.

Powder-based 3D printing should not cause any dimensional changes while fabricating the scaffolds and should print the scaffolds in designed dimensions. Moreover, features of 3D printing machine is to give high mechanical strength to

the biomaterial and to print the scaffolds in regular shapes. However, the scaffolds were not in the regular shape and defined dimensions.

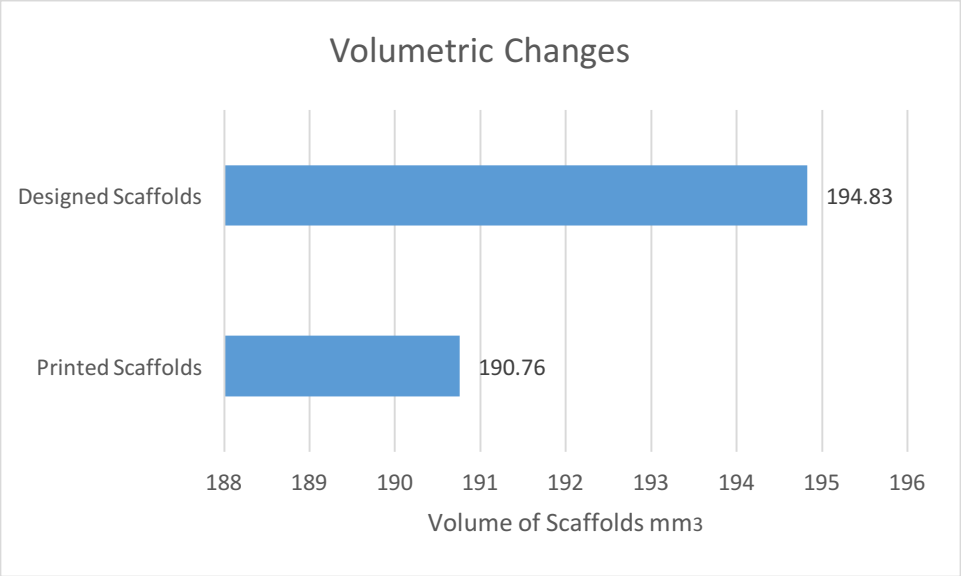

Figure 26: Volumetric changes of scaffolds after 3D printing process

Linear and Volumetric shrinkage of the defined dimensions and printed scaffolds can be seen in Table 3.

Table 3: Linear and Volumetric shrinkage of scaffolds after the fabrication process

SAMPLE	Linear Shrinkage	Volumetric Shrinkage
A-W Glass Ceramic Scaffold	-11.90%	2.09%

4.2 Effect of the Sintering Process

Green parts were sintered to enhance the densification and mechanical strength of the A-W glass ceramic scaffolds. During the sintering process, the binder burned out and left a porous structure. The green parts were black due to the ink but it burned out as well during the sintering process. The difference between the scaffolds before and sintering can be seen in Figure 27. The scaffolds swelled up and that caused even more shrinkage in the volume of A-W glass ceramic scaffolds.

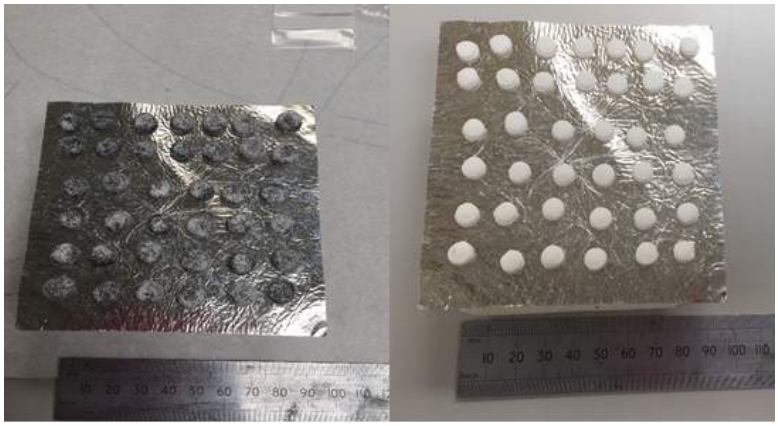

Figure 27: Non-sintered and sintered scaffolds

The sintering process led to the shrinkage of scaffolds because of exposing to the high temperature. Dimensions of the sintered scaffolds were measured digital caliper (Mitutoyo, UK). Dimensions of the green parts and sintered scaffolds could be seen in Appendix a and b. Linear and Volumetric shrinkage of the scaffolds were calculated by taking mean and standard deviation of calculations according to equation (1) and (2) that is shown in Table 4. Volume of the green parts were 190.348mm^3 when it was compared to sintered scaffolds, final volume of the scaffolds were 119.706 mm^3 (Table 4), all the calculations could be seen in appendix-d. A-W scaffolds had 37.12% of volumetric shrinkage which is a high dimension of shrinkage. It can be evaluated that the densification process made the scaffolds smaller. Sintering of the scaffolds increased the thickness as 13.80%. Theoretically, scaffolds shrink due to leading them to high temperatures. However, increasing in the thickness is not a usual result of the sintering process.

Table 4: Shrinkage percentages of scaffolds after sintering process

SAMPLE	Mean Linear Shrinkage	Mean Volumetric Shrinkage
A-W Glass Ceramic Scaffold	-13.80%	37.12%

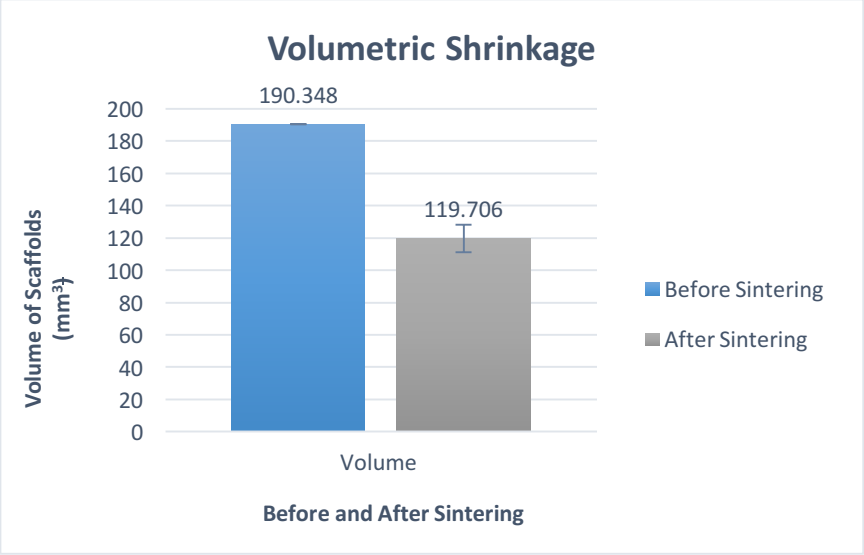

Figure 28: Volumetric shrinkage of scaffolds

4.3 Apparent Porosity

Interconnected porosity is crucial for scaffolds to provide nutrients and oxygen to the cells. If the scaffolds have a porous structure, degradation of the scaffolds is accomplished as well. However, the percentage of porosity is a key point to be gained suitable mechanical strength.

To be able to calculate porosity of the scaffolds, principally the scaffolds were weighed as dry, submerged and wet as Figure 21 and mass weights of the scaffolds can be seen in appendix-I. Apparent porosity of the scaffolds were 23% according to the equation (3).

4.4 Bioactivity Test

In vitro test had been perfomed to observe bioactivity and biodegradation of the scaffolds. A-W scaffolds had been soaked in SBF for 7, 14, 21, 28, 35, 42 days. SBF solution were refreshed in every 3 days to be able to provide pH value of human blood plasma. To evaluate the variation of the pH value of the SBF solution, it had been checked in every 3 days, all pH values in every 3 days could be seen in appendix-e. Changes in the pH value of the solution are based on dissolution of the minerals of A-W glass ceramic scaffolds such as Si, Ca and P. On the other hand bioactivity and biodegradation of the scaffold depends on the pH value of the solution as well.

According to Kokubo et al (2006), 7.3 ±1.5 of pH value is acceptable for SBF. The medium were prepared 4 times periodically, pH values of the solutions orderly; 7.35, 7.40, 7.54, 7.47. After refreshing the SBF solution in every 3 days, it had been observed that the value did not increase to the high levels. However, the scaffolds that reached to 7.84 pH value which were immersed for 10 days, it might be due to realizing of the ions of A-W scaffolds. SEM images would show that crystals were deposited on the surface of the scaffolds and it might affect the pH variation of the SBF solution as well. The pH value rose to 7.6 between 15^{th} and 29^{th} days of immersing in SBF solution.

One group of the scaffolds were immersed in SBF solution for 42 days without refreshing the solution. When the solution were prepared, the pH value was 7.35 and it could be seen in Figure 30 the pH value of SBF increased sharply. However, the value were stabilized between 5^{th} and 15^{th} days of immersion. Fluctuations of the pH value can be seen clearly due to calibrating the pH meter wrong. Theoretically, the value of pH should be stable after 5 days of immersion.

The pH variation of the scaffolds immersed in SBF 7, 14, 21, 28, 35, 42 days with refreshing the solution in every 3 days can be seen in Figure 29 and the group of scaffolds were immersed in SBF for 42 days without refreshing the solution can be seen in Figure 30.

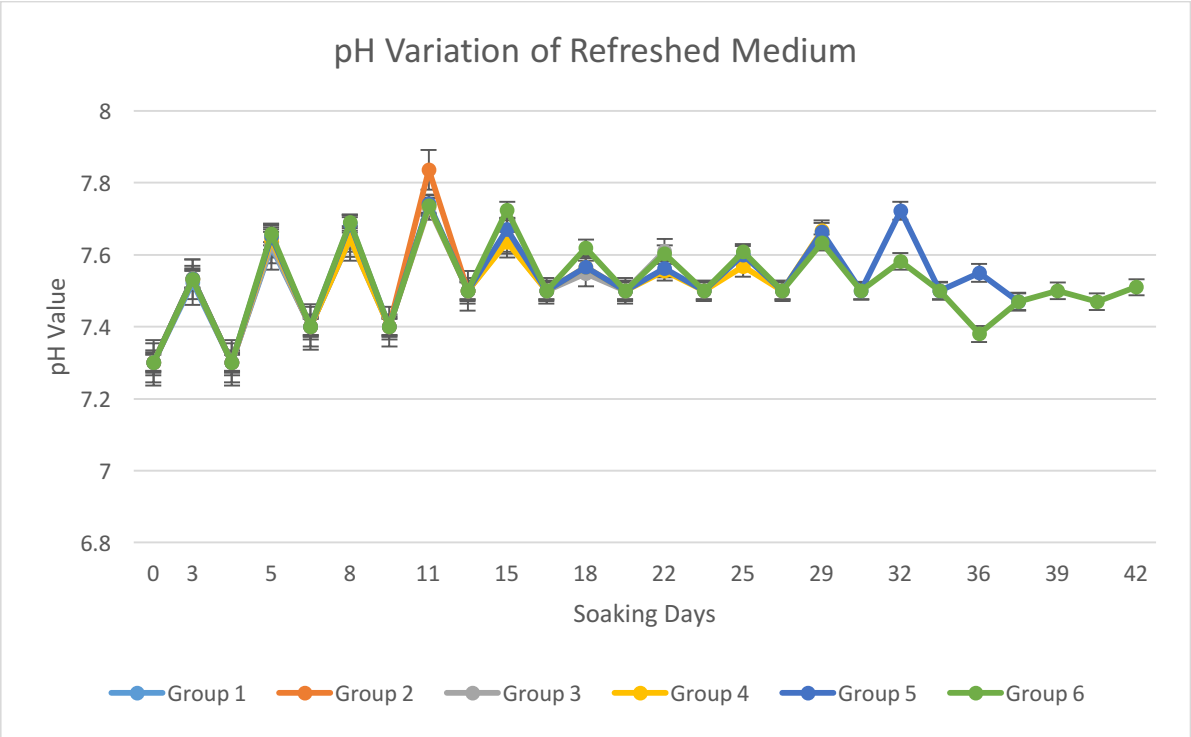

Figure 29: pH variation of Refreshed SBF solution for 6 weeks samples

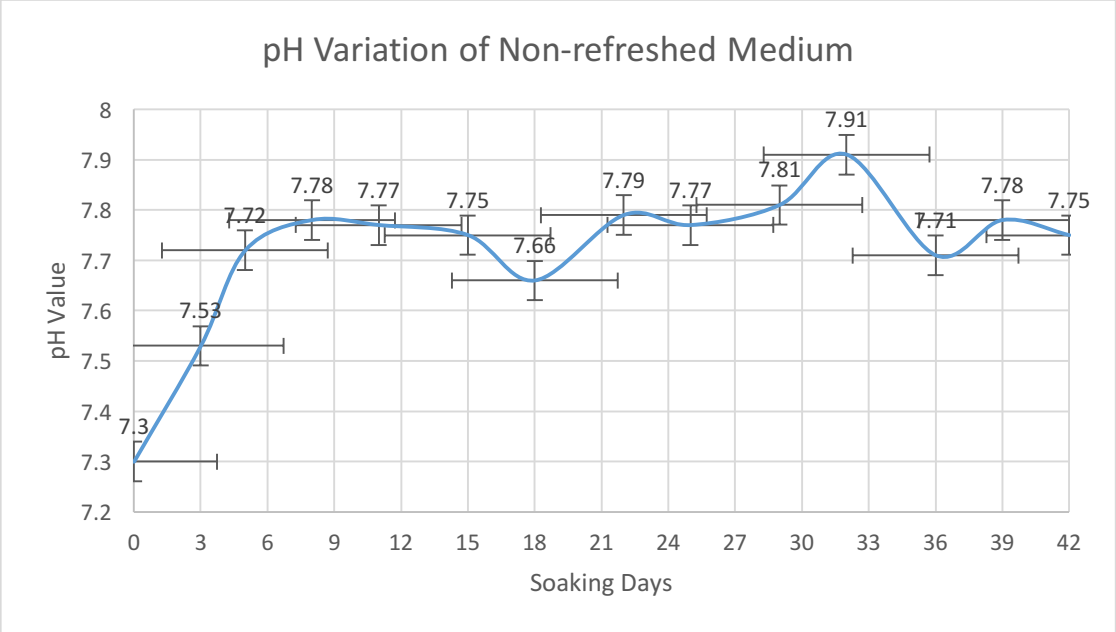

Figure 30: pH variation of non-refreshed SBF

4.5 Mass Loss Evaluation

Biodegradation of the scaffolds could be analysed by mass loss. To be able to evaluate the mass loss the scaffolds, they were weighed before immersion in SBF then dry weight of the scaffolds were weighed periodically in 7th, 14th, 21st, 28th, 35th, 42nd days. Thus, mass loss were calculated taking the difference of the weight of the scaffolds which were not immersed and the weight of the scaffolds which were soaked in SBF (appendix-f-g).

In Figure 31, 0.05 % of mass loss could be seen after immersing in SBF for 1 week. However, 0.22 % of sharp increment were calculated in weight of the scaffolds in second week of immersion in the solution. Increasing of the weights were slightly less in the scaffolds that they were soaked in SBF for three and four weeks. In third week weight of the scaffolds were increased 0.06% and increment in weight of the scaffolds were 0.01% that soaked in SBF for four weeks.

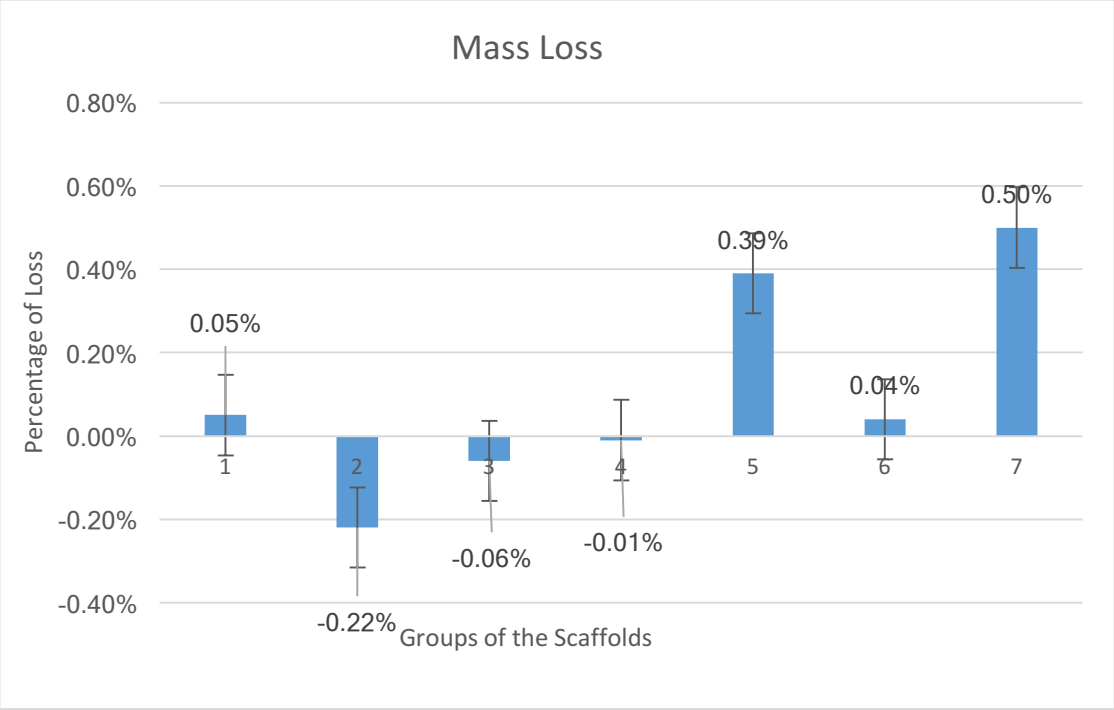

Figure 31: Mass loss percentages of the scaffolds that immersed in SBF for 1,2,3,4,5,6,7 weeks

4.6 Characterisation of the Scaffolds

Surface microstructure of scaffolds were observed with SEM for 7, 14, 21, 28, 35, 42 days in different magnifications such as x100, x150, x500, x1000 and x1500 to be able to observe apatite-like layer on the surface of the scaffolds and to measure pore sizes of the scaffolds.

4.6.1 Analysing of Apatite-like layer

Various sections of the surface of the scaffolds were analysed under SEM to observe the formation of apatite-like layer and bioactivity of the scaffolds would be examined. Samples were removed from SBF solution in 7^{th}, 14^{th}, 21^{st}, 28^{th}, 35^{th}, 42^{nd} days as weekly. Zero-day samples were not soaked in SBF to compare the effect of the SBF solution. Another comparison were performed by not refreshing medium for 42 days (7 weeks). Results of the characterisation can be seen below.

Surface morphology of the scaffold which was not soaked in SBF could be seen in Figure 32. Surface of the scaffold is smooth and porous. Any apatite-like layer formation were not observed.

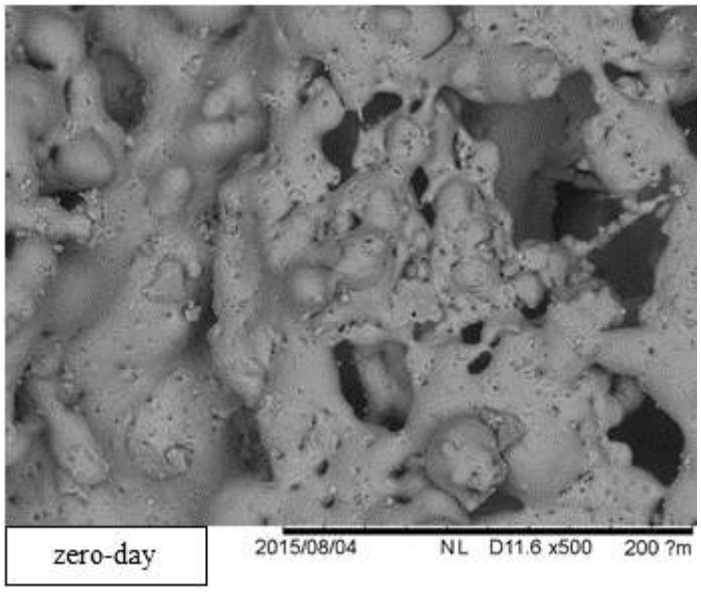

Figure 32: SEM images of the non-immersed scaffold in SBF

The image of the SEM (

Figure 33) shows that the scaffold had not any apatite minerals on the surface during immersion for 7 days. Only some crystal particles could be seen on the surface.

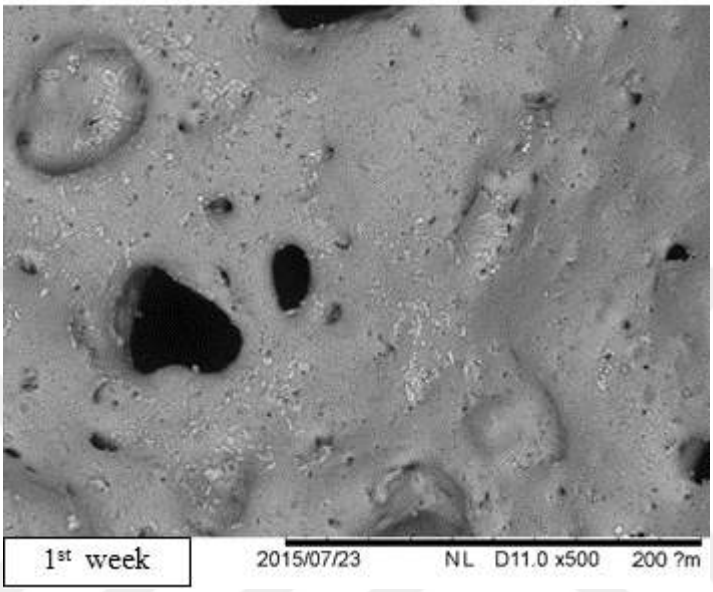

Figure 33: SEM images of the scaffold soaked in SBF for 7 days in SBF

The scaffold which was soaked for 14 days had growing crystallinity property that is shown in Figure 34 and small apatite minerals were observed as well.

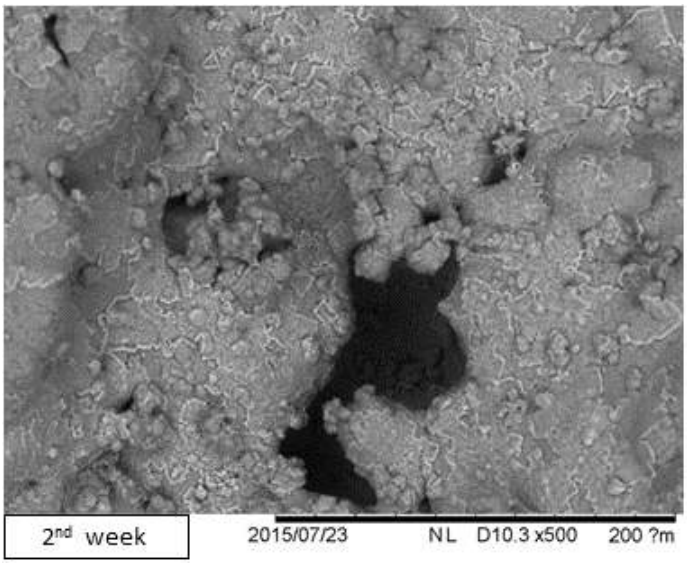

Figure 34: SEM images of the scaffold soaked for 14 days in SBF

Apatite-like layer could be seen clearly in Figure 35, the layer looks like buttons. Biodegradation of the scaffolds could be evaluated according to SEM image of the third week. Cracks occurred due to the stress on the free surface of the biomaterial.

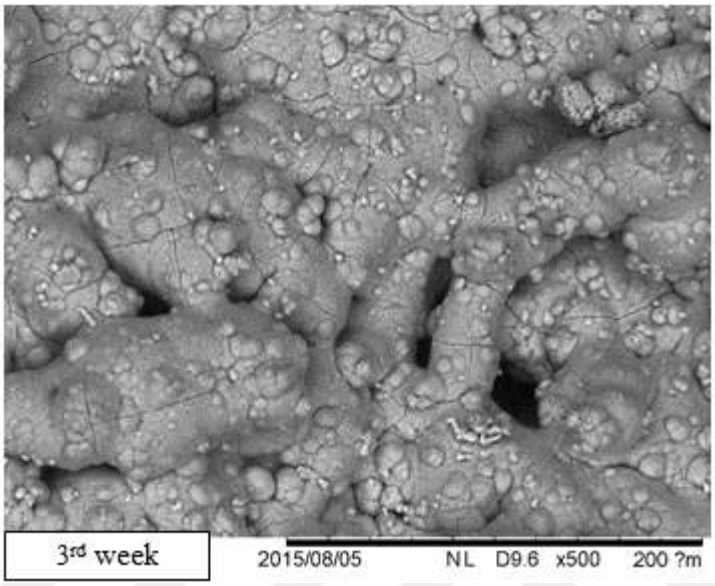

Figure 35: SEM images of the scaffolds for 21 days in SBF

The result of the SEM image of the scaffold that soaked for 28 days in SBF shows that apatite like layer started to cover the surface and cracks could be observed.

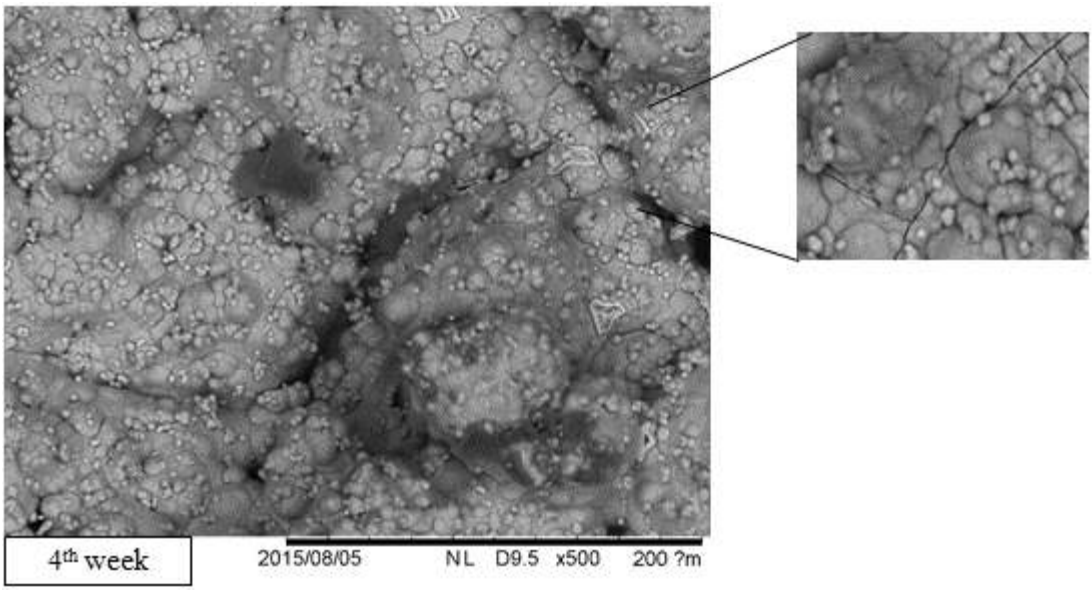

Figure 36: SEM images of the scaffolds for 28 days in SBF

The surface morphologies of the scaffolds which were soaked in SBF for 35 and 42 days could be seen in Figure 37 and Figure 38. Crack formation and needle-like structures were observed. Deposition of the apatite-like layer covered the surface of the scaffolds.

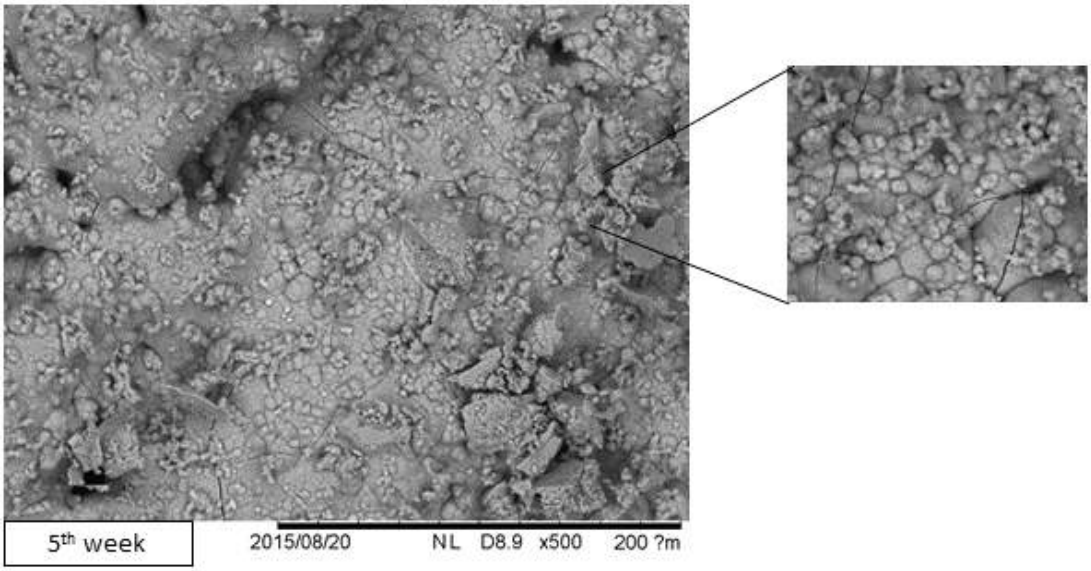

Figure 37: SEM images of the scaffold soaked for 35days in SBF

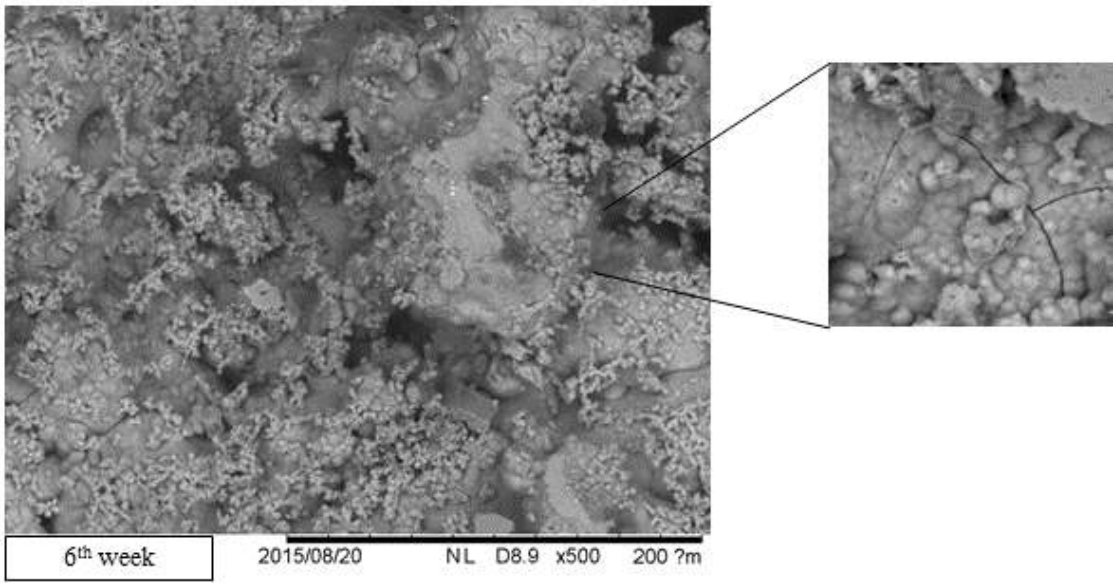

Figure 38: SEM images of the scaffolds soaked for 42 days in SBF

Figure 39 shows that any apatite-like layer were not deposited on surface of the scaffolds which were be soaking in non-refreshed medium for 42 days. However, glassy particles could be seen on the surface.

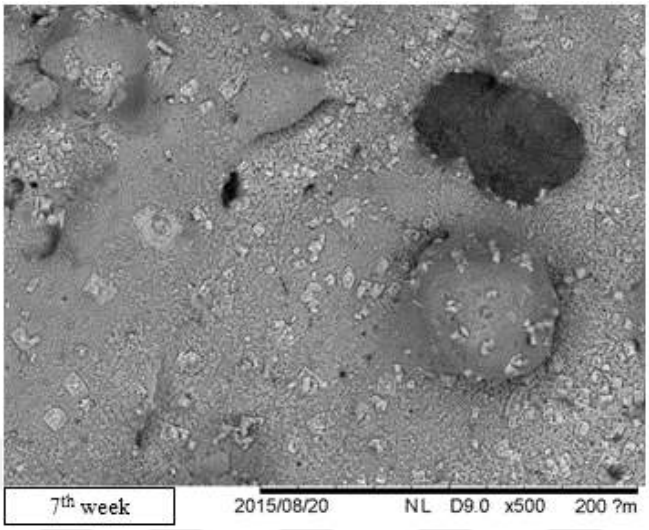

Figure 39: SEM images of the scaffold soaked for 42 days in SBF without refreshing

4.6.2 Pore Size of the Scaffolds

Sizes of the pores should be 100μm as minimum to be able sustain bone regeneration and transfer nutrients. Moreover, to provide a maximum efficiency for tissue ingrowth pore size should be between 200 and 350 μm.

Porous structures of the scaffolds were analyzed with SEM to measure pore sizes. Figure 40 shows that the largest pore size of the scaffolds were 150μ.

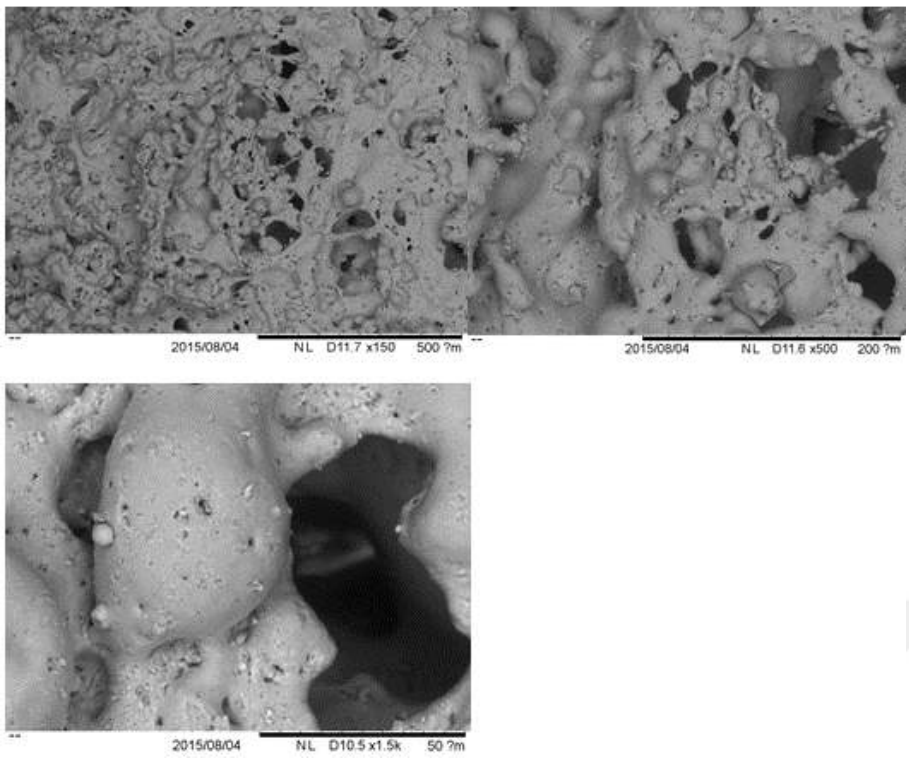

Figure 40: SEM images of the porous scaffold

5 DISCUSSION

Apatite- wollastonite were chosen as the reinforcing phase due to its high mechanical strength which is better than ceramics and glasses. To provide efficient mechanical and biological properties, a composite material is desired which is crucial for bone tissue engineering to be able to sustain load bearing and tissue ingrowth. Moreover, it has similar minerals such as hydroxyapatite with the main inorganic minerals of the bone structure. Thus, it is biodegradable, bioactive and non-toxic.

5.1 3D printing fabrication process

Additive manufacturing techniques are novel methods to fabricate complex geometrical designs easily and fastly. These techniques have been attracted attentions especially for scaffold fabrications since traditional techniques require labour intensive process, have long fabrication process, poor repeatability and it is challenging to create uniform shapes with regular shaped pores and dimensions. Therefore, in this study powder based 3D printing were chosen to

print A-W glass ceramic scaffolds and also it is an appropriate technique for glass ceramic scaffolds and cheap as well[29].

However, as it can be seen Figure 25 printed A-W scaffolds have distorted shape. Reasons of irregular shape of scaffolds might be powder packing density, powder flowability, layer thickness, binder drop volume, binder saturation and powder wettability[6]. All of the properties and requirement should be optimised prior to fabrication process. Principally, powder packing density depends on particle size distribution of the powder. Moreover, mechanical strength and porosity could be controlled with powder packing density as well. High packing density is obtained with mixing small particle size and large particle size which also sustain higher mechanical strength and porosity. Furthermore, powder packing density has an influence on printing process to enhance the quality of the scaffolds since bulk and tapped density depends on particle sizes and it has a remarkable impact on the quality of the powder bed. A flat, smooth, homogenous and compact powder bed is crucial to print mechanically strength, porous and uniformly shaped scaffolds. To obtain an effective powder bed placing the powder in the feed piston is crucial as well. Powder should be turned up with polypropylene scraper to remove air in the powder then surface of powder compact and smooth with a tamper. Thus, powder could be spread to build piston successfully without air in the powder. Powder flowability could be controlled by particle size, surface roughness, shape and size distribution and it is crucial to spread the powder onto build piston perfectly[6]. It is necessary for thin powder layers to build and also to remove the printed structures from the build piston. Geometry of designed structure and characteristic of powder affect the layer thickness and it could be controlled by these properties. Thin layers cause tolerance and poor resolution since the binder can penetrate easily to other sides. On the other hand, high saturation is necessary for thick layers to be able to bind powder to binder. Another property to improve the quality of the fabricated scaffold is wettability of powder which is associated with chemistry of particle and surface energy[6, 37].

Design of the scaffold which is architectural characteristic is one of the key points to sustain osteoconductivity, permeability, nutrient transport and vascularization and also affects mechanical strength as well.

In this study, some problems with the ink of 3D printings happened during the printing process and scaffolds could not be printed in the beginning. Therefore, it might have an effect on the shape of the scaffolds too. However, enough trials and re-printing could not be performed because of restricted-time experiment.

5.2 Shrinkage after printing the scaffolds

Scaffolds were designed in Inventor with defined dimensions as 10.25mm diameter and 2.25mm thickness. However, the actual size of printed scaffolds were in different dimensions as 9.52mm diameter and 2.68mm thickness. According to Huang 2015 et al., changing of material phase might cause to dimensional accuracy during 3D printing of structures. To prevent dimensional accuracy, Finite Element Analysis could be performed to predict the tolerance Huang, [38]. Dimensional accuracy affects pore size, porosity and interconnectivity in the scaffold [12].Therefore, it should be compensated prior to printing process.

5.3 Effect of Sintering Process

Post-processing is applied to sinter the green parts to increase the mechanical strength. Binder burns out during the sintering process and it gives a porous structure. However, dwelling time and temperature varies depend on the type of material. In this research work, glass ceramic scaffolds were sintered at 1150°C. Ceramics are brittle in high temperatures however the effect of glassy phase prevented cracking. Therefore, any fragile structure could not be observed while handling the structures.

Before sintering process volume of the composite were 190.348 mm^3, after sintering the green parts volume of scaffold was 119.706 mm^3. According to results of equation (1) and (2), linear shrinkage is -13.80% which means length of scaffolds increased and volumetric shrinkage is 37.12%. Volumetric shrinkage was developed due to densification of A-W/GC scaffolds.

Length of scaffolds rose because of crystallinity of hydroxyapatite and it can mostly be adjusted with sintering temperature[39]. Crystal structure could be increased with rising the temperature and it lowers the biodegradation rate[40]. Shrinkage usually occurs due to the evaporation of the water molecules which

is liquid binder. The compensation of shrinkage could be determine prior to post-processing to obtain sufficient final dimensions of the composite.

5.4 Porosity Evaluation

Pores are crucial to sustain nutrition and oxygen to cells and to get out waste. Bone regeneration and biomaterial degradation is enhanced in relation of increasing porosity. On the other hand, mechanical strength of scaffolds should be as high as bone strength and it decreases with increasing of porosity. Therefore, suitable porosity percentage should be gained. The open porosity is known as interconnected porosity and it is calculated by liquid displacement which is Archimedes' principle as it calculated in equation (3). The fraction of volume of the scaffold were filled with water in the pores structures[41]. According to Zilberman, 2011 et al., appropriate porosity value should be more than 80%. Moreover, Karageorgiou and Kaplan 2005 et al., defined the suitable porosity as between 40-90% for biomaterials that is for bone tissue to be able to sustain osteointegration between bone and implant and to provide biodegradation as well[25]. In this study, the obtained AW/GC scaffolds had 25% open porosity resulted in equation (3). The reason could be grain size of the powder which was 53μm. Porosity of the biomaterial varies depending on grain size and particle-size distribution of the scaffold [42]. Hence, to be able to obtain high porosity, smaller particle size could be used to fabricate the scaffolds and as it has been discussed in above parts, if small particles are mixed with large parts, high percentage porosity are obtained. Moreover, sintering process might affect the percentage of porosity as well. When the scaffolds is densified, porosity of the biomaterial decreases.

5.5 Bioactivity Test

Bioactivity is defined as interaction of biomaterial with host cell when it is implanted into the body. Bioactivity tests were performed in SBF solution in vitro study. If the scaffold is bioactive, silica-rich gel layer forms on the surface and apatite-like layer develops on the silica gel layer during the immersing days. Thickness of apatite layer becomes thicker increasing the immersion time in SBF solution[43]. Bioactivity test provides to analyse pH fluctuation and mass loss of scaffolds. Biodegradation of A-W glass ceramic scaffolds were analysed

measuring the pH value in every three days and weighing the dry weight of the scaffolds in 7^{th}, 14^{th}, 21^{st}, 28^{th}, 35^{th}, 42^{nd} days.

5.5.1 pH Variation

It had been observed that, pH value of SBF was prone to increase and when it was refreshed, the level of pH were decreased to pH value of the prepared medium (Figure 29). SBF solution were prepared 3 times as 1000mL and had been prepared in different pH values as 7.3, 7.42 and 7.47. Figure 29 shows that pH level did not increase to high values. Only in 2 weeks the pH value had a sharp peak to 7.8 value. It was reported that bioactive glass scaffold leads increment in the pH of the solution in the initial[15].

Non-refreshed SBF graph indicates increasing of pH value after immersing of scaffolds for 5 days and it continued as stable in the following days. However, there is a fluctuation between 15 and 18 days. Possibly, pH meter were calibrated wrong since the graph should be stable.

According to Kennedy 2005 et al., ion release and solubility was lower after soaking the dense HA in SBF for 32 days. After soaking for 35 days, pH value of the medium became acidic. Thus, It could be determined that increasing in pH was happened because of ion exchanges between Ca^{+} and H^{+} in the medium and it is led to be alkalized[44-46].

5.5.2 Mass Loss

Mass loss of scaffolds shows the biodegradation rate. Biodegradation of the scaffolds should not be too slow or fast to provide load bearing to the bone. Degradation must be at the same rate as tissue ingrowth[47, 48]. Scaffolds were taken out from the SBF solution periodically and they had been dried at ambient temperature for two days. Mass loss were calculated according to dry weight of the reference scaffolds which is before immersing in SBF solution. Mass loss of scaffolds could be observed in 7 days. However, after 1 week of soaking the scaffolds in the SBF solution, mass weights of scaffolds started to increase (Figure 31). Furthermore, weight of scaffolds should be decreasing. Reason of increasing of the scaffolds might be development of apatite-like layer on the surface of A-W glass ceramic scaffolds. 1^{st} week of immersion of the scaffolds in SBF solution, mass loss were analysed. However, deposition of apatite-like

layer might be much faster than degradation of scaffolds. Therefore, after observation of mass loss, the dry weight of the scaffolds sharply increased in 2nd week. Increment of the dry weight of the scaffolds which were soaked in SBF for 21 days were slightly less than 2nd week, it might be due to enhancement of degradation of scaffolds. In 28th day, degradation of the scaffolds and formation of the apatite-like layer were almost in balanced. Mass loss could be analysed evidently in 35th and 42nd of days. 6th group of the scaffolds which was immersed for 42 days in SBF had lower mass loss than expected. However, pH variation showed that decreasing of pH value might affect degradation rate of the scaffolds. The scaffolds that soaked in SBF for 42 days without refreshing the medium had highest mass lost percentage. Studies analysed that high surface area increases resorbability of material[22]. However, A-W glass ceramic scaffolds had small and irregular shapes. Therefore, biodegradation rate would not be as high as expected.

5.6 Characterisation of Scaffolds

5.6.1 Surface Morphology of the Scaffolds

Surface morphology of A-W glass ceramic composites were weekly analysed by SEM. the surface analysis of the scaffolds before and after soaking in SBF for 7, 14, 21, 28, 35, 42 days and the one group which were not immersed in SBF solution.

Any apatite-like layer or silica gel layer could not be observed on the surface of the scaffolds that were before soaking in SBF that is showed in Figure 32 and surface of the scaffold is smooth. Crystals appeared on the surface of the scaffolds as small needle aggregates while immersion in SBF for 7 days in Figure 33. After immersion of 14 days, crystal particles became bigger and some apatite minerals had been seen Figure 34. Furthermore, in third week image Figure 35 apatite like layer could be seen clearly and surface of A-W scaffolds had been started to crack. Cracks proved that A-W glass ceramic scaffolds degraded in SBF solution after 15 days of immersion.

It was reported that, cracks occur on the surface of the scaffolds due to the decomposition of Ca and Si ions from the glassy stage induced stress on the free surface of the scaffold and caused to the development of cracks[42]. Apatite

minerals had been forming increasingly comparing to Figure 34. Furthermore, deposition of the apatite-like layer and formation of cracks could be seen in Figure 36 as well. Figure 37 and Figure 38 showed that denser apatite minerals were examined and according to observations of the various sections of the scaffolds, apatite minerals covered the whole surface. Thickness of the apatite-like layer and concentration of the minerals such as Ca, Si and P could not be measured by EDS because of short time of experimental work.

However, it can be discussed that cracks showed that it had been degrading while the immersing time after 10 days. A-W glass ceramic scaffolds showed bioactive properties having formation of apatite like layer on the surface. According to Kennedy et al, the release of P and Ca ions from the composite rise the nucleation and deposition rate of apatite-like layer on the surface of the glass ceramic scaffold[7].

As discussion, in vitro tests and SEM analysis showed that pH value rose after 10 days of immersion in SBF, mass weight of the scaffolds increased and crystals appeared on the surface of the scaffolds and it might be silica-rich gel layer as well. It means biodegradation of the scaffolds were slower that development of the apatite-like layer.

5.6.2 Pore size of the Scaffolds

SEM analysis showed that the scaffolds did not have pore sizes more than 150μm. A-W glass ceramic scaffolds have the minimum pore size ranges. However, to be able to sustain all the requirements, efficient pore sizes ranges between 250-350 μm.

6 FUTURE WORKS

To be able to obtain efficient results, A-W glass ceramic scaffolds should be printed again. Volumetric changes due to printing the scaffolds and shrinkage effect of sintering process should be determined prior to fabrication procedure. Layer thickness should be considered as well to print regular shaped scaffolds. In this study, mechanical test could not be applied because of irregular distorted shape of the scaffolds. In future work, the compression test could be performed to identify elastic modulus and compressive strength by the stress-strain

diagram. In vitro tests showed that there are still some studies to be done to have accurate data for scaffolds.

7 CONCLUSION

As it has been discussed in literature review section, the scaffolds were printed quick and easily. However, regular shapes could not be obtained. Moreover, powder-based 3D printing should not have any effect on the dimensions of the scaffolds but designed and printed scaffolds had different volumes. Printed scaffolds were post-processed at high temperature to sinter the green parts. MD powder burned out in the first stage then scaffolds were sintered in the second stage of heat treatment.

Burned out powder created a porous structure. Porosity evaluation showed that the scaffolds had 25% of open porosity that is actually too low to be able to sustain all the requirements for bone regeneration. In vitro tests were showed that A-W glass ceramic scaffolds are bioactive biomaterials. According to SEM analysing, apatite-like layer were observed on the surface of the glass ceramic scaffolds. Biodegradation were determined after soaking for a week then mass weight of the scaffolds started to increase due to faster deposition of apatite-like layer than degradation of the scaffolds. After soaking for 35 days, mass weight of the scaffolds were started to decrease. Therefore, mass loss could be seen clearly in 7^{th}, 35^{th} and 42^{nd} days with and without refreshed. Degradation rate, bioactivity and mechanical strength of scaffolds are affected from the surface morphology and material compositions[49, 50]. Previous studies showed that after ion exchange, silica-rich gel layer forms and during the immersion time it starts to breakdown and resolve then repolymerization of the the apatite-like layer forms[46, 47, 51].

8 REFERENCES

1. Goodridge RD, Dalgarno KW and Wood DJ. Indirect selective laser sintering of an apatite-mullite glass-ceramic for potential use in bone replacement applications. *Proceedings of the Institution of Mechanical Engineers, Part H: Journal of Engineering in Medicine*. 2006; 220: 57-68.
2. Hutmacher DW, Sittinger M and Risbud MV. Scaffold-based tissue engineering: rationale for computer-aided design and solid free-form fabrication systems. *TRENDS in Biotechnology*. 2004; 22: 354-62.
3. Hofmann S and Garcia-Fuentes M. *Bioactive scaffolds for the controlled formation of complex skeletal tissues*. INTECH Open Access Publisher, 2011.
4. orthobullets. Fracture Healing. In: Medical L, (ed.).
5. Oryan A, Alidadi S and Moshiri A. Current concerns regarding healing of bone defects. *Hard tissue*. 2013; 2: 13.
6. Bose S, Vahabzadeh S and Bandyopadhyay A. Bone tissue engineering using 3D printing. *Materials Today*. 2013; 16: 496-504.
7. Suwanprateeb J, Sanngam R, Suvannapruk W and Panyathanmaporn T. Mechanical and in vitro performance of apatite–wollastonite glass ceramic reinforced hydroxyapatite composite fabricated by 3D-printing. *Journal of Materials Science: Materials in Medicine*. 2009; 20: 1281-9.
8. Chen Q, Roether JA and Boccaccini AR. Tissue engineering scaffolds from bioactive glass and composite materials. *Topics in tissue engineering*. 2008; 4: 1-27.
9. AC C. Bone Tissue Engineering: Production of scaffolds. *Introdução Engenharia Biomédica Mestrado Integrado Engenharia Biomédica*. Universidade de Lisboa, 2007.
10. Dawson JI and Oreffo ROC. Clay: new opportunities for tissue regeneration and biomaterial design. *Advanced Materials*. 2013; 25: 4069-86.
11. Bose S, Roy M and Bandyopadhyay A. Recent advances in bone tissue engineering scaffolds. *Trends in biotechnology*. 2012; 30: 546-54.
12. Salgado AJ, Coutinho OP and Reis RL. Bone tissue engineering: state of the art and future trends. *Macromolecular bioscience*. 2004; 4: 743-65.
13. Tarawneh AM, Wettergreen M and Liebschner MAK. Computer-aided tissue engineering: benefiting from the control over scaffold micro-architecture. *Computer-Aided Tissue Engineering*. Springer, 2012, p. 1-25.
14. Butscher A, Bohner M, Hofmann S, Gauckler L and Müller R. Structural and material approaches to bone tissue engineering in powder-based three-dimensional printing. *Acta Biomaterialia*. 2011; 7: 907-20.
15. Sabree I. Fabrication of bioactive glass scaffolds by stereolithography for bone tissue engineering. 2014.
16. Chen AA, Tsang VL, Albrecht DR and Bhatia SN. 3-D fabrication technology for tissue engineering. *BioMEMS and Biomedical Nanotechnology*. Springer, 2007, p. 23-38.
17. Liebschner MAK and Wettergreen MA. Optimization of bone scaffold engineering for load bearing applications. *Topics in tissue engineering*. 2003: 1-39.
18. Sabir MI, Xu X and Li L. A review on biodegradable polymeric materials for bone tissue engineering applications. *Journal of Materials Science*. 2009; 44: 5713-24.
19. Malowney D. The Shock Absorbers of the Spine. 2015.
20. Organisation IO. Introduction to Bone Biology: All About Our Bones. International Osteoporosis Organisation, 2015.
21. Yun H-s, Kim S-H, Khang D, Choi J, Kim H-h and Kang M. Biomimetic component coating on 3D scaffolds using high bioactivity of mesoporous bioactive ceramics. *International journal of nanomedicine*. 2011; 6: 2521.
22. El-Ghannam A, Hart A, White D and Cunningham L. Mechanical properties and cytotoxicity of a resorbable bioactive implant prepared by rapid prototyping technique. *Journal of Biomedical Materials Research Part A*. 2013; 101: 2851-61.

23. Loh QL and Choong C. Three-dimensional scaffolds for tissue engineering applications: Role of porosity and pore size. *Tissue Engineering Part B: Reviews*. 2013; 19: 485-502.
24. Yang S, Leong K-F, Du Z and Chua C-K. The design of scaffolds for use in tissue engineering. Part I. Traditional factors. *Tissue engineering*. 2001; 7: 679-89.
25. Karageorgiou V and Kaplan D. Porosity of 3D biomaterial scaffolds and osteogenesis. *Biomaterials*. 2005; 26: 5474-91.
26. Chu PK and Liu X. *Biomaterials fabrication and processing handbook*. CRC press, 2008.
27. Sanson O. Scaffolds ceramici da polimero preceramico tramite stampante 3D. Preceramic polymer-derived ceramic scaffolds by 3D-printing. 2013.
28. Ashby and Jones. EduPack, Level 2. 2014.
29. Lam CXF, Mo XM, Teoh S-H and Hutmacher DW. Scaffold development using 3D printing with a starch-based polymer. *Materials Science and Engineering: C*. 2002; 20: 49-56.
30. Sun W, Starly B, Nam J and Darling A. Bio-CAD modeling and its applications in computer-aided tissue engineering. *Computer-aided design*. 2005; 37: 1097-114.
31. Sachlos E and Czernuszka JT. Making tissue engineering scaffolds work. Review: the application of solid freeform fabrication technology to the production of tissue engineering scaffolds. *Eur Cell Mater*. 2003; 5: 39-40.
32. Subia B, Kundu J and Kundu SC. *Biomaterial scaffold fabrication techniques for potential tissue engineering applications*. INTECH Open Access Publisher, 2010.
33. Lorrison JC, Dalgarno KW and Wood DJ. Processing of an apatite-mullite glass-ceramic and an hydroxyapatite/phosphate glass composite by selective laser sintering. *Journal of Materials Science: Materials in Medicine*. 2005; 16: 775-81.
34. Hollister SJ. Porous scaffold design for tissue engineering. *Nature materials*. 2005; 4: 518-24.
35. Reay S, Withell AJ and Grupp I. Porous ceramic filters through 3d printing. 2011.
36. Kokubo T and Takadama H. How useful is SBF in predicting in vivo bone bioactivity? *Biomaterials*. 2006; 27: 2907-15.
37. Butscher A. Powder based three-dimensional printing of calcium phosphate structures for scaffold engineering. Diss., Eidgenössische Technische Hochschule ETH Zürich, Nr. 21210, 2013, 2013.
38. Huang Q, Zhang J, Sabbaghi A and Dasgupta T. Optimal offline compensation of shape shrinkage for three-dimensional printing processes. *IIE Transactions*. 2015; 47: 431-41.
39. Faeghi-Nia A. Preparation of Apatite-Wollastonite-Phlogopite glass-ceramic composites by powder sintering method. *Science of Sintering*. 2013; 45: 331-9.
40. Conz MB, Granjeiro JM and Soares GdA. Hydroxyapatite crystallinity does not affect the repair of critical size bone defects. *Journal of Applied Oral Science*. 2011; 19: 337-42.
41. Narayan R. *Biomedical materials*. Springer Science & Business Media, 2009.
42. Spath S, Drescher P and Seitz H. Impact of Particle Size of Ceramic Granule Blends on Mechanical Strength and Porosity of 3D Printed Scaffolds. *Materials*. 2015; 8: 4720-32.
43. Park J and Ozturk A. Bioactivity Of Apatite–Wollastonite Glass-Ceramics Produced By Melting Casting. *Surface Review and Letters*. 2013; 20: 1350010.
44. Silver IA, Deas J and Erecińska M. Interactions of bioactive glasses with osteoblasts in vitro: effects of 45S5 Bioglass®, and 58S and 77S bioactive glasses on metabolism, intracellular ion concentrations and cell viability. *Biomaterials*. 2001; 22: 175-85.
45. Miguel BS, Kriauciunas R, Tosatti S, et al. Enhanced osteoblastic activity and bone regeneration using surface-modified porous bioactive glass scaffolds. *Journal of Biomedical Materials Research Part A*. 2010; 94: 1023-33.

46. Mozafari M, Rabiee M, Azami M and Maleknia S. Biomimetic formation of apatite on the surface of porous gelatin/bioactive glass nanocomposite scaffolds. *Applied Surface Science*. 2010; 257: 1740-9.
47. Jones JR, Tsigkou O, Coates EE, Stevens MM, Polak JM and Hench LL. Extracellular matrix formation and mineralization on a phosphate-free porous bioactive glass scaffold using primary human osteoblast (HOB) cells. *Biomaterials*. 2007; 28: 1653-63.
48. Rahaman MN, Day DE, Bal BS, et al. Bioactive glass in tissue engineering. *Acta biomaterialia*. 2011; 7: 2355-73.
49. Coleman NJ, Bellantone M, Nicholson JW and Mendham AP. Textural and structural properties of bioactive glasses in the system CaO-SiO2. *Ceramics-Silikáty*. 2007; 51: 1-8.
50. Davison KS, Siminoski K, Adachi JD, et al. Bone strength: the whole is greater than the sum of its parts. *Seminars in arthritis and rheumatism*. Elsevier, 2006, p. 22-31.
51. Saravanapavan P, Jones JR, Pryce RS and Hench LL. Bioactivity of gel–glass powders in the CaO-SiO2 system: A comparison with ternary (CaO-P2P5-SiO2) and quaternary glasses (SiO2-CaO-P2O5-Na2O). *Journal of Biomedical Materials Research Part A*. 2003; 66: 110-9.

9 APPENDIXES

Appendix-A

1. 5 of 40 samples were chosen to estimate average dimensions of the printed scaffolds before printing process

Diameter of the scaffolds before sintering (mm)

	Diameters					
	Sample 1	Sample 2	Sample 3	Sample 4	Sample 5	**Mean**
	9.19	10.12	9.54	9.63	9.76	
	9.35	9.23	9.65	9.34	9.28	
	9.26	9.25	9.59	10.19	9.39	
Mean	9.26667	9.53333	9.59333	9.72	9.47667	9.518
SD	0.06549	0.41492	0.04497	0.3528	0.20532	0.2167

Thickness

	Sample 1	Sample 2	Sample 3	Sample 4	Sample 5	**Mean**
	2.81	2.52	2.29	2.77	2.91	
	3.04	2.79	2.67	2.43	2.84	
	3.02	2.6	2.53	2.6	2.41	
Mean	2.95667	2.63667	2.49667	2.6	2.72	2.682
SD	0.10403	0.11324	0.15691	0.1388	0.22106	0.14681

Appendix-B

2. Results of the average dimensions of 5 samples of 40 A-W glass ceramic scaffolds after sintering process

Dimensions of scaffolds after sintering process (mm)

Diameters

	Sample 1	Sample 2	Sample 3	Sample 4	Sample 5	**Mean**
	6.6	7.45	6.9	7.01	6.98	
	7.1	7.27	7.31	7.42	7.43	
	6.98	6.88	7.03	6.98	6.74	
Mean	6.89333	7.2	7.08	7.13667	7.05	7.072
SD	0.21312	0.23791	0.17108	0.20072	0.28601	0.221767

	Thickness					
	Sample 1	Sample 2	Sample 3	Sample 4	Sample 5	**Mean**
	2.91	3.01	3.35	3.35	3.38	
	2.77	2.57	3.06	2.97	3.22	
	2.89	2.97	3.25	3.17	2.91	
Mean	2.85667	2.85	3.22	3.16333	3.17	3.052
SD	0.06182	0.19866	0.12028	0.15521	0.19511	0.146215

Appendix-C

3. Results of linear shrinkage of 5 samples of A-W glass ceramic scaffolds

Shrink Percentage (Thickness) %

Sample 1	**Sample 2**	**Sample 3**	**Sample 4**	**Sample 5**
	-	-	-	-
3.38218715	8.091024	28.971963	21.666667	16.544118

Appendix-D

4. Results of Volume calculations of the scaffolds before and after sintering process

Volume of cylinder is calculated by;

$$Volume\ of\ cylinder\ = \pi \times r^2 \times h$$

Where r is radius of the scaffold, h is height of the scaffold

Volume of the scaffolds before sintering (mm^3)

S1	S2	S3	S4	S5	**Mean**	**SD**
199.67	186.58	180.58	192.92	191.99	190.348	6.415959

Volume of Sintered Scaffold(m

S1	S2	S3	S4	S5	**Mean**	**SD**
106.63	116.04	126.77	126.52	122.57	119.706	7.602033

Appendix-E

5. pH Values of the scaffolds for every 3 days.

d Day 8.7.2015

oup 1	**S1**	**S2**	**S3**	**S4**	**S5**	**Mean**	**SD**
	7.51	7.53	7.51	7.54	7.53	**7.524**	**0.012**
oup 2	**S1**	**S1**	**S2**	**S3**	**S5**		
	7.55	7.54	7.5	7.52	7.55	**7.532**	**0.01939072**
oup 3	**S1**	**S2**	**S3**	**S4**	**S5**		
	7.53	7.54	7.53	7.53	7.54	**7.534**	**0.00489898**
oup 4	**S1**	**S2**	**S3**	**S4**	**S5**		

	7.52	7.55	7.53	7.54	7.53	**7.534**	**0.01019804**
oup 5	**S1**	**S2**	**S3**	**S4**	**S5**		
	7.53	7.54	7.55	7.53	7.52	**7.534**	**0.01019804**
oup 6	**S1**	**S2**	**S3**	**S4**	**S5**		
	7.52	7.53	7.55	7.54	7.52	**7.532**	**0.0116619**
oup 7	**S1**	**S2**	**S3**	**S4**	**S5**		
	7.53	7.52	7.52	7.53	7.55	**7.53**	**0.01095445**

4th Day 10.07.2015

Group 1	**S1**	**S2**	**S3**	**S4**	**S5**	**Mean**	**SD**
	7.6	7.63	7.63	7.62	7.63	**7.622**	**0.0116619**
Group 2	**S1**	**S2**	**S3**	**S4**	**S5**		
	7.62	7.63	7.62	7.65	7.64	**7.632**	**0.0116619**
Group 3	**S1**	**S2**	**S3**	**S4**	**S5**		
	7.63	7.64	7.6	7.63	7.64	**7.628**	**0.01469694**
Group 4	**S1**	**S2**	**S3**	**S4**	**S5**		
	7.64	7.65	7.63	7.64	7.65	**7.642**	**0.00748331**
Group 5	**S1**	**S2**	**S3**	**S4**	**S5**		
	7.65	7.66	7.65	7.65	7.65	**7.652**	**0.004**

Group 6	S1	S2	S3	S4	S5		
	7.67	7.65	7.64	7.67	7.66	**7.658**	**0.0116619**
Group 7	**S1**	**S2**	**S3**	**S4**	**S5**		
	7.7	7.73	7.7	7.72	7.73	**7.716**	**0.01356466**

8th Day 14.07.2015

Group 1	**S1**	**S2**	**S3**	**S4**	**S5**	**Mean**	**SD**
Collected	7.61	7.64	7.63	7.68	7.67	**7.646**	**0.0257682**
Group 2	**S1**	**S2**	**S3**	**S4**	**S5**		
	7.62	7.64	7.64	7.67	7.68	**7.65**	**0.0219089**

Group 3	**S1**	**S2**	**S3**	**S4**	**S5**		
	7.63	7.64	7.6	7.67	7.68	**7.644**	**0.0287054**
Group 4	**S1**	**S2**	**S3**	**S4**	**S5**		
	7.6	7.64	7.67	7.68	7.64	**7.646**	**0.028**

Group 5	S1	S2	S3	S4	S5		
	7.67	7.68	7.68	7.7	7.7	**7.686**	**0.012**
Group 6	**S1**	**S2**	**S3**	**S4**	**S5**		
	7.72	7.71	7.6	7.7	7.72	**7.69**	**0.04560702**
Group 7	**S1**	**S2**	**S3**	**S4**	**S5**		
	7.77	7.74	7.79	7.81	7.78	**7.778**	**0.02315167**

10th Day 17.07.2015

Group 2	S1	S2	S3	S4	S5	Mean	SD
	7.83	7.84	7.84	7.83	7.84	**7.836**	**0.00489898**
Group 3	**S1**	**S2**	**S3**	**S4**	**S5**		
	7.7	7.74	7.74	7.74	7.74	**7.732**	**0.016**
Group 4	**S1**	**S2**	**S3**	**S4**	**S5**		
	7.73	7.73	7.74	7.74	7.74	**7.736**	**0.00489898**
Group 5	**S1**	**S2**	**S3**	**S4**	**S5**		
	7.73	7.74	7.75	7.74	7.75	**7.742**	**0.00748331**
Group 6	**S1**	**S2**	**S3**	**S4**	**S5**		

	7.73	7.74	7.74	7.73	7.74	**7.736**	**0.00489898**
Group 7	**S1**	**S2**	**S3**	**S4**	**S5**		
	7.76	7.78	7.76	7.78	7.76	**7.768**	**0.00979796**

14th Day- 21.08.2015

	S1	**S2**	**S3**	**S4**	**S5**	**Mean**	**SD**
Group 2	7.62	7.64	7.63	7.67	7.68	**7.648**	**0.02315167**
	S1	**S2**	**S3**	**S4**	**S5**		
Group 3	7.63	7.64	7.6	7.64	7.68	**7.638**	**0.0256125**
	S1	**S2**	**S3**	**S4**	**S5**		
Group 4	7.63	7.64	7.63	7.64	7.64	**7.636**	**0.00489898**
	S1	**S2**	**S3**	**S4**	**S5**		
Group 5	7.67	7.68	7.68	7.68	7.64	**7.67**	**0.01549193**
	S1	**S2**	**S3**	**S4**	**S5**		
Group 6	7.7	7.68	7.7	7.76	7.78	**7.724**	**0.03878144**
	S1	**S2**	**S3**	**S4**	**S5**		
Group 7	7.74	7.75	7.75	7.76	7.76	**7.752**	**0.00748331**

17th Day –
24.07.2015

	S1	S2	S3	S4	S5	Mean	SD
Group3	7.58	7.54	7.54	7.53	7.55	**7.548**	**0.01720465**

	S1	S2	S3	S4	S5		
Group 4	7.6	7.54	7.55	7.6	7.54	**7.566**	**0.028**

	S1	S2	S3	S4	S5		
Group 5	7.6	7.63	7.55	7.5	7.55	**7.566**	**0.04498889**

	S1	S2	S3	S4	S5		
Group 6	7.64	7.63	7.6	7.63	7.6	**7.62**	**0.0167332**

	S1	S2	S3	S4	S5		
Group 7	7.74	7.75	7.72	7.5	7.6	**7.662**	**0.09724197**

21st Day- 28

.07.2015

	S1	S2	S3	S4	S5	Mean	SD
Group 3	7.63	7.61	7.61	7.61	7.59	**7.61**	**0.01264911**
	S1	**S2**	**S3**	**S4**	**S5**		
Group 4	7.54	7.55	7.58	7.59	7.52	**7.556**	**0.0257682**
	S1	**S2**	**S3**	**S4**	**S5**		
Group 5	7.58	7.55	7.56	7.54	7.58	**7.562**	**0.016**
	S1	**S2**	**S3**	**S4**	**S5**		
Group 6	7.62	7.58	7.63	7.63	7.56	**7.604**	**0.0287054**
	S1	**S2**	**S3**	**S4**	**S5**		
Group 7	7.78	7.78	7.79	7.81	7.81	**7.794**	**0.01356466**

25th Day-

31.07.2015

	S1	S2	S3	S4	S5	Mean	SD
Group 4	7.5	7.59	7.55	7.6	7.6	**7.568**	**0.03867816**
	S1	**S2**	**S3**	**S4**	**S5**		
Group 5	7.63	7.6	7.57	7.58	7.62	**7.6**	**0.02280351**
	S1	**S2**	**S3**	**S4**	**S5**		
Group 6	7.63	7.62	7.59	7.58	7.62	**7.608**	**0.01939072**
	S1	**S2**	**S3**	**S4**	**S5**		
Group 7	7.78	7.75	7.76	7.78	7.79	**7.772**	**0.01469694**

29th Day- 04.08.2015

						Mean	SD
	S1	**S2**	**S3**	**S4**	**S5**		
Group 4	7.67	7.69	7.65	7.66	7.67	**7.668**	**0.0132665**
	S1	**S2**	**S3**	**S4**	**S5**		
Group 5	7.67	7.65	7.67	7.65	7.68	**7.664**	**0.012**
	S1	**S2**	**S3**	**S4**	**S5**		
Group 6	7.6	7.64	7.65	7.63	7.65	**7.634**	**0.01854724**
	S1	**S2**	**S3**	**S4**	**S5**		
Group 7	7.81	7.8	7.79	7.83	7.8	**7.806**	**0.01356466**

32nd Day- 08.08.2015

						Mean	SD
	S1	**S2**	**S3**	**S4**	**S5**		
Group 5	7.67	7.7	7.73	7.75	7.76	**7.722**	**0.03310589**
	S1	**S2**	**S3**	**S4**	**S5**		
Group 6	7.52	7.59	7.6	7.62	7.58	**7.582**	**0.0337046**
	S1	**S2**	**S3**	**S4**	**S5**		
Group 7	7.93	7.91	7.88	7.92	7.89	**7.906**	**0.01854724**

36th Day- 11.08.2015

						Mean	SD
	S1	**S2**	**S3**	**S4**	**S5**		
Group 5	7.56	7.58	7.53	7.52	7.56	**7.55**	**0.0244949**
	S1	**S2**	**S3**	**S4**	**S5**		
Group 6	7.4	7.35	7.36	7.38	7.4	**7.378**	**0.02280351**
	S1	**S2**	**S3**	**S4**	**S5**		
Group 7	7.72	7.68	7.73	7.71	7.74	**7.716**	**0.02302173**

39th Day- 14.08.2015

						Mean	SD
	S1	**S2**	**S3**	**S4**	**S5**		
Group 6	7.5	7.5	7.47	7.53	7.5	**7.5**	**0.01897367**
	S1	**S2**	**S3**	**S4**	**S5**		
Group 7	7.74	7.76	7.81	7.79	7.79	**7.778**	**0.02481935**

42nd Day- 17.08.2015

						Mean	SD
	S1	**S2**	**S3**	**S4**	**S5**		
Group 6	7.53	7.5	7.52	7.5	7.52	**7.514**	**0.012**
	S1	**S2**	**S3**	**S4**	**S5**		
Group 7	7.75	7.73	7.75	7.75	7.75	**7.746**	**0.008**

Appendix-F

6. Mass weights of the scaffolds before soaking in SBF

Group 1

	Sample 1	**Sample 2**	**Sample 3**	**Sample 4**	**Sample 5**	**Mean**
	0.1802	0.1895	0.1762	0.1826	0.1829	
	0.18	0.1893	0.176	0.1825	0.185	
	0.1798	0.1895	0.1762	0.1824	0.1849	
Mean	0.18	0.18943333	0.17613333	0.1825	0.18426667	**0.182466667**
SD	0.000163299	9.4281E-05	9.4281E-05	8.16497E-05	0.00096724	**0.00028015**

Group 2

	Sample 1	Sample2	Sample 3	Sample 4	Sample 5	Mean
	0.1838	0.1817	0.1816	0.1898	0.1889	
	0.1839	0.1818	0.1817	0.1898	0.1887	
	0.1839	0.1817	0.1817	0.1897	0.1888	
Mean	0.183866667	0.18173333	0.18166667	0.189766667	0.1888	**0.185166667**
SD	4.71405E-05	4.714E-05	4.714E-05	4.71405E-05	8.165E-05	**5.40423E-05**

Group 3

	Sample 1	Sample 2	Sample 3	Sample 4	Sample 5	Mean
	0.175	0.182	0.1931	0.1879	0.1696	
	0.1749	0.1819	0.193	0.1879	0.1693	
	0.175	0.182	0.193	0.188	0.1694	
Mean	0.174966667	0.18196667	0.19303333	0.187933333	0.16943333	**0.181466667**
SD	4.71405E-05	4.714E-05	4.714E-05	4.71405E-05	0.00012472	**6.26567E-05**

Group 4

	Sample 1	Sample 2	Sample 3	Sample 4	Sample 5	Mean
	0.187	0.1884	0.1746	0.1899	0.1878	
	0.1869	0.1884	0.1745	0.1899	0.1879	
	0.1869	0.1883	0.1747	0.1899	0.1878	
Mean	0.186933333	0.18836667	0.1746	0.1899	0.18783333	**0.185526667**
SD	4.71405E-05	4.714E-05	8.165E-05	2.77556E-17	4.714E-05	**4.46142E-05**

Group 5

	Sample 1	Sample 2	Sample 3	Sample 4	Sample 5	Mean
	0.1854	0.1872	0.1742	0.1918	0.1919	
	0.1853	0.1873	0.1746	0.1919	0.1918	
	0.1854	0.1873	0.1747	0.1918	0.1918	
Mean	0.18536667	0.18726667	0.1745	0.19183333	0.19183333	**0.18**
SD	4.714E-05	4.714E-05	0.000216025	4.714E-05	4.714E-05	**8.0917E**

Group 6

	Sample 1	Sample 2	Sample 3	Sample 4	Sample 5	Mean
	0.1897	0.1852	0.1921	0.1875	0.1858	
	0.1898	0.1853	0.1919	0.1874	0.1856	
	0.1898	0.1853	0.192	0.1875	0.1587	
Mean	0.18976667	0.18526667	0.192	0.18746667	0.1767	**0.18**
SD	4.714E-05	4.714E-05	8.16497E-05	4.714E-05	0.01272818	**0.00259**

Group 7

	Sample 1	Sample 2	Sample 3	Sample 4	Sample 5	Mean
	0.1833	0.1793	0.1906	0.181	0.186	
	0.1833	0.1794	0.1906	0.1809	0.186	
	0.1833	0.1794	0.1906	0.1808	0.1861	
Mean	0.1833	0.17936667	0.1906	0.1809	0.18603333	**0.18**
SD	0	4.714E-05	0	8.165E-05	4.714E-05	**3.5186E**

Appendix-G

7. Dry weight of the scaffolds after soaking in SBF for 7, 14, 21, 28, 35, 42 days.

Group 1

	Sample 1	Sample 2	Sample 3	Sample 4	Sample 5	Mean
	0.17997	0.18945	0.17603	0.18235	0.18465	
	0.17941	0.18900	0.17664	0.18201	0.1844	
	0.17921	0.18967	0.17640	0.18279	0.18422	
Mean	0.17953	0.18937	0.17636	0.18238	0.18442	**0.18241**
SD	0.0003217	0.0002788	0.0002509	0.0003193	0.000176	**0.00026941**

Group 2

	Sample 1	Sample 2	Sample 3	Sample 4	Sample 5	Mean
	0.1844	0.1823	0.182	0.1901	0.1893	
	0.1842	0.182	0.1819	0.1901	0.1893	
	0.1843	0.1822	0.1818	0.1901	0.1892	
Mean	0.1843	0.1821667	0.1819	0.1901	0.189267	**0.18554667**
SD	8.165E-05	0.0001247	8.165E-05	2.776E-17	4.71E-05	**6.7032E-05**

Group 3

Sample 1	Sample 2	Sample 3	Sample 4	Sample 5	Mean
0.1696	0.1879	0.1932	0.1828	0.1746	

	0.1697	0.188	0.1933	0.1827	0.1746	
	0.1696	0.1879	0.1932	0.1827	0.1745	
Mean	0.1696333	0.1879333	0.1932333	0.1827333	0.174567	**0.18162**
SD	4.714E-05	4.714E-05	4.714E-05	4.714E-05	4.71E-05	**4.714E-05**

Group 4

	Sample 1	**Sample 2**	**Sample 3**	**Sample 4**	**Sample 5**	**Mean**
	0.187	0.1882	0.1745	0.19	0.1881	
	0.1871	0.1881	0.1743	0.1899	0.188	
	0.187	0.1882	0.1746	0.1898	0.1881	
Mean	0.1870333	0.1881667	0.1744667	0.1899	0.188067	**0.18552667**
SD	4.714E-05	4.714E-05	0.0001247	8.165E-05	4.71E-05	**6.9559E-05**

Group 5

	Sample 1	**Sample 2**	**Sample 3**	**Sample 4**	**Sample 5**	**Mean**
	0.1844	0.1872	0.1743	0.1892	0.1919	
	0.1845	0.1873	0.1743	0.1892	0.1918	
	0.1845	0.1873	0.1744	0.1892	0.1919	
Mean	0.184466667	0.18726667	0.17433333	0.1892	0.19186667	**0.185426667**
SD	4.71405E-05	4.714E-05	4.714E-05	0	4.714E-05	**3.77124E-05**

Group 6

	Sample 1	Sample 2	Sample 3	Sample 4	Sample 5	Mean
	0.1848	0.1895	0.1847	0.1871	0.185	
	0.1847	0.1897	0.1845	0.1871	0.1849	
	0.1847	0.1896	0.1843	0.1871	0.1848	
Mean	0.184733333	0.1896	0.1845	0.1871	0.1849	**0.186166667**
SD	4.71405E-05	8.165E-05	0.0001633	0	8.165E-05	**7.47478E-05**

Group 7

	Sample 1	Sample 2	Sample 3	Sample 4	Sample 5	Mean
	0.1825	0.1783	0.1898	0.1795	0.1856	
	0.1825	0.1784	0.1899	0.1795	0.1853	
	0.1824	0.1785	0.1897	0.1793	0.1856	
Mean	0.182466667	0.1784	0.1898	0.179433333	0.1855	**0.18312**
SD	4.71405E-05	8.165E-05	8.165E-05	9.42809E-05	0.00014142	**8.92284E-05**

Appendix-I

8. Dry, submerged and wet weight of the scaffolds

Dry Weight

	Sample 1	Sample 2	Sample 3	Sample 4	Sample 5	Mean
	0.1915	0.1806	0.1893	0.1864	0.1887	
	0.192	0.1807	0.1892	0.1868	0.1892	
	0.1919	0.1809	0.1893	0.1866	0.1888	
Mean	0.1918	0.18073333	0.18926667	0.1866	0.1889	0.18
SD	0.00021602	0.00012472	4.714E-05	0.0001633	0.00021602	0.00015

Suspended in Water

	Sample 1	Sample 2	Sample 3	Sample 4	Sample 5	Mean
	0.1132	0.1086	0.1106	0.1102	0.1105	
	0.1139	0.1045	0.1109	0.1081	0.1104	
	0.1137	0.1049	0.1111	0.1078	0.1103	
Mean	0.1136	0.106	0.11086667	0.1087	0.1104	0.10991
SD	0.00029439	0.00184572	0.00020548	0.00106771	8.165E-05	0.00069

	Wet Weight					
	Sample 1	**Sample 2**	**Sample 3**	**Sample 4**	**Sample 5**	**Mean**
	0.2241	0.2076	0.2252	0.212	0.2138	
	0.2148	0.2019	0.2188	0.2076	0.2094	
	0.2112	0.1974	0.2114	0.2063	0.2011	
Mean	0.2167	0.2023	0.21846667	0.20863333	0.2081	0.210
SD	0.00543507	0.00417373	0.00563875	0.00243903	0.00526561	0.004590